HHS Public Access

Author manuscript

Dev Biol. Author manuscript; available in PMC 2016 October 01.

Published in final edited form as:

Dev Biol. 2015 October 1; 406(1): 74–91. doi:10.1016/j.ydbio.2015.06.022.

Rap1 GTPase is required for mouse lens epithelial maintenance and morphogenesis

Rupalatha Maddala[1], **Tharkika Nagendran**[1], **Richard A. Lang**[2], **Alexei Morozov**[3], and **Ponugoti V. Rao**[1,4,*]

[1]Department of Ophthalmology, Duke University School of Medicine, Durham, NC.27710 USA

[2]The Visual System Group, Division of Pediatric Ophthalmology and Developmental Biology, Children's Hospital Research Foundation, University of Cincinnati, Cincinnati, OH 45229, USA

[3]Virginia Tech Carilion Research Institute, Roanoke, Virginia. 24016. USA

[4]Department of Pharmacology and Cancer Biology, Duke University School of Medicine, Durham, NC. 27710. USA

Abstract

Rap1, a Ras-like small GTPase, plays a crucial role in cell-matrix adhesive interactions, cell-cell junction formation, cell polarity and migration. The role of Rap1 in vertebrate organ development and tissue architecture, however, remains elusive. We addressed this question in a mouse lens model system using a conditional gene targeting approach. While individual germline deficiency of either Rap1a or Rap1b did not cause overt defects in mouse lens, conditional double deficiency (Rap1 cKO) prior to lens placode formation led to an ocular phenotype including microphthalmia and lens opacification in embryonic mice. The embryonic Rap1 cKO mouse lens exhibited striking defects including loss of E-cadherin- and ZO-1-based cell-cell junctions, disruption of paxillin and β1-integrin-based cell adhesive interactions along with abnormalities in cell shape and apical-basal polarity of epithelium. These epithelial changes were accompanied by increased levels of α-smooth muscle actin, vimentin and N-cadherin, and expression of transcriptional suppressors of E-cadherin (Snai1, Slug and Zeb2), and a mesenchymal metabolic protein (Dihydropyrimidine dehydrogenase). Additionally, while lens differentiation was not overtly affected, increased apoptosis and dysregulated cell cycle progression were noted in epithelium and fibers in Rap1 cKO mice. Collectively these observations uncover a requirement for Rap1 in maintenance of lens epithelial phenotype and morphogenesis.

Keywords

Rap1 GTPase; Lens morphogenesis; Cell adhesion; Polarity; Epithelial plasticity

[*]**Correspondence:** P. Vasantha Rao, Ph.D, Department of Ophthalmology, Duke University School of Medicine, Durham, NC. 27710, Phone: 919-681-5883, Fax: 919-684-8983, p.rao@dm.duke.edu.

Introduction

Morphogenesis of vertebrate organs is critically dependent on temporally and spatially coordinated events including specialized cell-cell junction formation, cell-extracellular matrix (ECM) adhesive interactions, establishment of cell polarity and migration (Boettner and Van Aelst, 2009; Bulgakova et al., 2012; Franke, 2009; Nelson, 2009). Importantly, defects in these cellular characteristics can lead to various phenotypes and diseases (Franke, 2009; Halbleib and Nelson, 2006). Identifying the molecular mechanisms regulating cell adhesive interactions, cell polarity and migration is therefore not only necessary for disease understanding, but is also expected to provide novel insights for therapeutic manipulation of structural and functional defects in certain tissues and organs. Rap1 GTPase, a Ras-like small GTPase, is considered to be a crucial player in controlling formation and stability of E-cadherin- and ZO-1- based adherens junctions (AJ) and tight junctions (TJ), respectively, and integrin-mediated cell-ECM adhesion, cell polarity and migration (Asha et al., 1999; Boettner and Van Aelst, 2009; Glading et al., 2007; Hogan et al., 2004; Knox and Brown, 2002; Kooistra et al., 2007; Severson et al., 2009). Rap1 is a widely expressed small GTPase that integrates signals from external cues and receptors to regulate cell adhesive interactions, actin cytoskeletal reorganization and intracellular regulatory pathways (Boettner and Van Aelst, 2009; Kooistra et al., 2007). Analogous to other small GTPases, Rap1 acts as a molecular switch by cycling between inactive GDP-bound and active GTP-bound forms, with the transition between these two conformations being tightly controlled by specific guanine nucleotide exchange factors (GEFs) and GTPase-activating proteins (GAPs), respectively. Several multi-domain GEFs which activate Rap1 and cell junction formation have been identified and characterized, including C3G, Epacs, PDZ-GEFs, RapGAPs and DOCK4 (Gloerich and Bos, 2011). Likewise, a number of downstream effector proteins work in concert with Rap1 to regulate cell adhesive interactions, including afadin/AF6, KRIT/CCM1 and RIAM (Boettner et al., 2000; Glading et al., 2007; Liu et al., 2011; Mandai et al., 2013). Inhibition of Rap1 has been demonstrated to impair AJs formation and disrupt integrin-based cell adhesive interactions, and conversely, activation of Rap1 strengthens cell-cell junctions and cell adhesion (Kooistra et al., 2007). Cell-cell junctions (TJs, AJs) and integrin-linked focal adhesions are considered to be important sites for anchoring and organization of the actin cytoskeleton (Meng and Takeichi, 2009; Rikitake et al., 2012) (DeMali et al., 2003; Mitic and Anderson, 1998), and Rap1 has been demonstrated to regulate actin cytoskeletal organization at cell-cell junctions by controlling the activities of different Rho GTPases and myosin II (Ando et al., 2013; Arthur et al., 2004; Boettner and Van Aelst, 2007; Fukuyama et al., 2006; Jeon et al., 2007; Ogita and Takai, 2006). In our previous studies, although cell-cell junctions and cell adhesive interactions regulated by E-cadherin and N-cadherin (Lang et al., 2014; Pontoriero et al., 2009), and Rho GTPases were found to be crucial for lens development and morphogenesis (Chauhan et al., 2011; Maddala et al., 2011a; Maddala et al., 2008), the role of Rap1 in lens morphogenesis and architecture remains unexplored.

Moreover, although a vast amount of knowledge is available regarding the mechanisms by which Rap1 regulates cellular processes (Boettner and Van Aelst, 2009; Choi et al., 2013; Kooistra et al., 2007; Liu et al., 2011; O'Keefe et al., 2012; Sawyer et al., 2009), little is

known at large about Rap1 function in vertebrate organ development, morphogenesis and tissue architecture. Additionally, functional redundancy of the two isoforms of Rap1 (Rap1a and Rap1b) poses a major impediment for the ability to thoroughly delineate the biological role of Rap1 (Chrzanowska-Wodnicka, 2013; Frische and Zwartkruis, 2010; Li et al., 2007). Early attempts to explore Rap1 role in vertebrate morphogenesis and tissue architecture were also thwarted by embryonic lethality noted in model systems lacking both isoforms of Rap1 (Chrzanowska-Wodnicka et al., 2008; Li et al., 2007). Therefore, it is necessary to design a model system presenting conditional deficiency of Rap1 to determine how double deficiency of Rap1a and Rap1b might impact organ morphogenesis and tissue architecture. In this study we targeted Rap1 (Rap1a and Rap1b) expression in a conditional manner to identify the definitive and mechanistic role of Rap1 in ocular lens morphogenesis and architecture.

Vertebrate lens morphogenesis, which is initiated from a single cell type (Chow and Lang, 2001; Cvekl and Ashery-Padan, 2014; McAvoy et al., 1999), provides a unique model system to investigate the role of Rap1 regulated cell-cell junctions and cell adhesive interactions in the specification, polarization and proliferation of epithelial cells, their differentiation into fiber cells, and in the migration and arrangement of mature fiber cells. The ocular lens is an avascular transparent tissue with no innervation, comprised only of epithelial cells that continuously proliferate and differentiate into specialized fiber cells, all encased by a thick basement membrane, the lens capsule. The lens develops from ectoderm that overlies the optic vesicle, a process that involves transition of the surface ectoderm through the lens placode, pit and vesicle stages(McAvoy et al., 1999). At the lens vesicle stage, the posterior half of the cells elongate and differentiate into primary fibers, whereas cells in the anterior half differentiate into epithelial cells that cover the apical ends of the fiber cells and develop lens distinctive polarized structure. Proliferation in the adult lens is restricted to the epithelium, mostly in the germinative zone above the lens equator, and progeny migrate below the equator where they elongate and differentiate into secondary fiber cells that progressively become added to the primary fiber mass. Like primary fibers, secondary fibers are also highly polarized with their apical ends associated with the overlying epithelium and the posterior terminals attaching to the inner surface of the extracellular matrix-enriched elastic capsule. Since we possess a good understanding of the temporal sequence of events in lens morphogenesis (Chow and Lang, 2001; Cvekl and Ashery-Padan, 2014; Lovicu and McAvoy, 2005), here we sought to determine the role of Rap1 in lens development and architecture, using the developing lens as a model system for organogenesis. Rap1 deficient conditional mice (Rap1 cKO) generated in this study exhibit a lens phenotype at embryonic stages, epithelial plasticity and mesenchymal transition accompanied with loss of AJs and ZO-1-based cell junctions in conjunction with upregulation of E-cadherin suppressing transcription factors, demonstrating the requirement of Rap1 in the establishment and maintenance of epithelial phenotype and morphogenesis of lens.

Materials and Methods

Animal Maintenance and Use

Animals were maintained in a pathogen-free vivarium under a 12 hour dark and light cycle with ad libitum food and water. All experiments using mice were carried out in accordance with the recommendations of the Guide for the Care and Use of Laboratory Animals of the National Institutes of Health and the Association for Research in Vision and Ophthalmology. The protocol was approved by the Committee for Ethics of Animal Experiments at the Duke University School of Medicine. At required gestational ages, fetuses were removed by hysterectomy after the dams had been anesthetized with Euthasol.

Rap1a and Rap1b null mouse eyes

Eyes from adult Rap1a$^{-/-}$ (Li et al., 2007) and Rap1b$^{-/-}$ (Chrzanowska-Wodnicka et al., 2008) null mice on a C57BL/6 genetic background, fixed in 3.7% buffered formalin, were generously provided by the laboratories of Magdalena Chrzanowska-Wodnicka from the Blood Research Institute, Blood Center of Wisconsin, Milwaukee, WI., and Lawrence Quilliam from the Department of Biochemistry and Molecular Biology, Indiana University of School of Medicine, Indianapolis, IN, respectively.

Generation of Rap1 (Rap1a/Rap1b) GTPase conditional deficient mice

To generate Rap1a/Rap1b double conditional deficient mice (Rap1 cKO), the well characterized Rap1a and Rap1b homozygous double floxed mice (Rap1a^{ff}/Rap1b^{ff} with 129S/C57BL6 mixed background; Listed in the Jackson Laboratory as strain B6;129S-*Rap1a*^{tm1Morz} *Rap1b*^{tm1Morz}/J) described earlier (Pan et al., 2008) were mated with Le-Cre transgenic mice (C57BL6 background). The resulting heterozygous offspring were inbred for 4 generations, until we could generate the progeny carried with Rap1a^{ff}/Rap1b^{ff}/Cre genotype. The homozygous double floxed Rap1a^{ff}/Rap1b^{ff} mice used in this study contain loxp sites flanking exon 2–3 (in Rap1a) and exon-1 (in Rap1b) and are viable, fertile and do not display any abnormalities (Pan et al., 2008). Le-Cre transgenic mice used in this study express Cre recombinase at embryonic day 8.75 under the control of a Pax6 P0 enhancer/promoter, with Cre being expressed in lens epithelium and fiber cells as well as other surface ectoderm-derived eye structures (Ashery-Padan et al., 2000). The Le-Cre mice also express a Cre-activatable GFP reporter that is incorporated into the Cre transgene. For comparison with Rap1 cKO mice, we used age-matched Le-Cre transgenic and wild type (WT) mice (C57BL/6 background) as controls. Collected tail biopsies from progeny were screened for the Rap1a/Ra1b floxed alleles and Cre transgene by PCR analysis using the respective specific primers (Table S1) as described earlier by us (Maddala et al., 2011a; Pan et al., 2008).

Histological analysis

Rap1cKO mouse embryos were obtained from timed mated pregnant females at 10.5, 11.5, 13.5, 15.5, 17.5 days of gestation. The embryonic heads and whole eyes (from postnatal day 1(P1)) mice were fixed for 2 hours at room temperature in 50 mM cacodylate buffer (pH 7.2) containing 2.5% glutaraldehyde, 4% sucrose and 2 mM $CaCl_2$, and transferred to 3.7%

buffered formalin for 24 hours. Rap1cKO and WT specimens were subsequently dehydrated, embedded in paraffin, and cut in 5μm thick sections with a microtome (Leica Leitz model no.1512), prior to staining with hematoxylin and eosin (H&E). Images were captured using Zeiss Axio Imager equipped with a Hamamatsu Orca ER monochrome CCD camera.

Immunofluorescence

For immunostaining tissue specimens were dissected out, fixed with 3.7% buffered formalin for 24 hours, dehydrated, embedded in paraffin and 5μm thick sections were cut as we described earlier (Maddala et al., 2011a). De-paraffinization and antigen retrieval were performed as we described earlier (Maddala et al., 2011b). These tissue sections were blocked for 10 minutes in a humidified chamber with the medical background Sniper reducing solution (BiocareMedical, Concord, CA), prior to incubation for 24 hours at 4°C, with a 1:200 dilution of one of the following primary antibodies: Rap1 (Cell Signaling Technologies, Danvers, MA), E-cadherin (Cell Signaling Technologies), β-catenin (monoclonal, Sigma-Aldrich, St Louis, MO), N-cadherin (monoclonal, Invitrogen, Camarillo CA) and Slug (Sigma-Aldrich). Tissue sections were washed in TBS buffer (Tris buffered saline) and incubated in a dark humidified chamber for 2 hours at room temperature, with either Alexa fluor 488 or 594 conjugated secondary antibodies (Invitrogen, Grand Island, NY; at a 1: 200 dilution) following which, sections were washed again with TBS buffer and incubated with Hoechst 33342 (1:1000 dilutions, Life Technologies, Grand Island, NY), for 10 minutes. Slides were mounted using Vecta mount and nail polish and micrographs captured using a Nikon Eclipse 90i confocal laser scanning microscope as we described earlier (Maddala et al., 2011a).

For staining of activated β1-integrin, WT and Rap1cKO embryo heads were fixed in IHC Zinc fixative (BD Pharmingen, San Jose, CA) for 24 hours and processed as mentioned above. The de-paraffinized tissue sections were incubated with anti-rat β1integrin antibody (clone 9EG7 from BD Pharmingen) at 1:25 dilution.

For cryosectioning, WT and Rap1 cKO embryo heads were fixed in 4% buffered paraformaldehyde for 24 hours at 4°C, transferred into 5% and 30% sucrose in PBS on successive days (phosphate buffered saline), embedded in Optimal Cutting Temperature (OCT) embedding media (Tissue-Tek, Torrance, CA) and cut into 8–10 μm thick sections before being immunostained as we described earlier (Maddala et al., 2011a). Briefly, air dried tissue cryosections were treated with Image-iT® FX signal enhancer (Invitrogen, Eugene, OR) and blocked using blocking buffer (5% globulin free bovine serum albumin, 5% filtered goat serum in 0.3% TritonX100 containing PBS) for 30 minutes each, prior to overnight incubation at 4°C with one of the following primary antibodies in blocking buffer (at a 1:200 dilution): phospho-paxillin (Tyr118), ZO-1 (both from Cell Signaling Technologies), anti-GFP conjugated to Alexa fluor 488 (Life technologies, Grand Island, NY), vimentin, γ-crystallin and aquaporin-0 (generously provided by Roy Quinlan, Durham University, UK., Sam Zigler, Johns Hopkins University School of Medicine and Joe Horwitz, Jules Stain Eye Institute, UCLA, respectively). Sections were then washed in wash buffer (0.3% Tritin-X100 containing PBS) and incubated with Alexa Fluor secondary

antibodies. For F-actin and α-smooth muscle actin staining, preblocked sections were labeled with phalloidin conjugated with tetra rhodamine isothiocyanate (TRITC) (500 ng/ml) or α-smooth muscle actin monoclonal antibody conjugated with Cy3™ (both from Sigma-Aldrich) for 2 hours, washed and mounted as described above. All representative immunofluorescence data reported in this study are based on analysis of a minimum of 4 to 6 tissue sections derived from three independent specimens per group.

Immunoblotting

To evaluate changes in protein levels of Rap1(Rap1a/Rap1b) GTPase, aPKCλ and aPCKς, lenses derived from E17.5 embryos of WT and Rap1 cKO mice (4 lenses pooled per sample) were homogenized in Tris (10 mM) buffer pH 7.4 containing 0.2 mM $MgCl_2$, 5 mM N-Ethylmaleimide, 2.0 mM sodium orthovanadate, 10 mM sodium fluoride, 60 μM phenyl methyl sulfonyl fluoride, 0.4 mM iodoacetamide and Protease inhibitor cocktail tablets (complete, Mini, EDTA free and PhosSTOP Phosphatase Inhibitor Cocktail Tablets, 1 each/ 10ml buffer, Roche-Basel, Switzerland). Homogenates were centrifuged at 800×g for 10 minutes at 4 °C, and the supernatant fractions were centrifuged further at 100,000×g for 1 hour at 4 °C. The 100,000×g supernatant was designated as the soluble fraction, while the insoluble pellet was re-suspended in Tris buffer (described above), washed twice with the same buffer prior to suspending the final membrane-enriched protein pellet in urea buffer containing 8 M urea, 20 mM Tris, 23 mM glycine, 10 mM dithiothreitol, and saturated sucrose along with protease and phosphatase inhibitors. Protein concentration was estimated using Bio-Rad reagent (Bio-Rad, Cat. 500-0006). Equal amounts of membrane enriched fractions (for Rap1) or total (800×g) fractions (for aPKC) were resolved on 12% SDS-PAGE gels, followed by electrophoretic transfer to nitrocellulose membrane, overnight incubation with Rap1or aPKCλ or aPKCζ antibodies at 1:1000 dilution in TBS buffer containing 5% milk and 0.1 Tween-20, washing and incubation with peroxidase-conjugated secondary antibody. Immunoblots were developed by enhanced chemiluminescence (ECL), and scanned densitometrically using a Foto Dyne Gel Doc scanner equipped with TL100 software. Densitometry analyses were carried out using Image J software.

RT-PCR and qRT-PCR analysis

To detect the expression of Rap1a, Rap1b, C3G, Epac, GAPs, GDS, and downstream Rap1 effector proteins nectin and afadin in P2 and P24 normal mouse (C57BL6 genetic background) lenses, total RNA was extracted from pooled lenses using an RNeasy Micro kit (Qiagen, Valencia, CA) per manufacturer protocol. The Advantage RT-for-PCR Kit (Clontech, Mountain View, CA) was used to synthesize first-strand cDNA from total RNA, followed by amplification of cDNA pools for the genes of interest, using an Advantage® 2 PCR Kit (Clontech, Mountain View, CA) and the respective oligonucleotide primer sets (Table S1). Gene amplification was performed using a C1000 Touch™ Thermal Cycler (Bio-Rad, Hercules, CA) with a denaturation step at 95°C for 0 seconds, followed by annealing at 60°C for 0 seconds and extension at 72°C for 60 seconds. The cycle was repeated 25–30 times with a final step at 72°C for 5 minutes. The amplified gene products were separated on 2% agarose gels, stained with ethidium bromide and imaged with a Fotodyne Trans-illuminator (Fotodyne, Inc, Hartland, WI). The resolved bands were excised and sequenced for gene identification.

For qRT-PCR analysis, total RNA was isolated from the lenses of E17.5 embryos of WT and Rap1cKO mice and single stranded cDNA synthesis was performed as described above. The qRT-PCR reactions were set up for Rap1a, Rap1b, Snail, Slug, dihydropyrimidine dehydrogenase (DPYD), Zeb1 and Zeb2 genes using a Prism 7700 Sequence Detection System (Applied Biosystem, Inc; Grand Island, NY) and the respective specific oligonucleotide primer sets (Table S1). Fold differences in gene expression between the WT and Rap1cKO mouse lenses were normalized to GAPDH and calculated by the comparative threshold (CT) method, as described by the manufacturer.

TUNEL assay

Wild type and Rap1cKO mouse lens cryosections derived from E15.5 and E17.5 embryos were used for detecting apoptotic cells by in situ terminal transferase dUTP nick end labeling (TUNEL) using an ApopTag Plus Fluorescein kit (Chemicon, S7111, Temecula, CA) and Nikon Eclipse 90i confocal laser scanning microscope as we described earlier (Maddala et al., 2011a). Green/yellow labelled apoptotic positive cells were scored in the lens epithelium and fibers of 6 independent specimens from both WT and Rap1 ckO specimens and quantitated.

BrdU incorporation

Timed mated pregnant WT and Rap1cKO mice at day 15.5 post-conception, were injected with bromo-deoxy-uridine (BrdU) at a concentration of 100 μg/gram body weight and were sacrificed after two hours of incorporation as we described earlier (Maddala et al., 2008). Embryo heads were fixed for cryosectioning (Maddala et al., 2008). After genotyping, 8–10 μm thick serial sections were cut and used for BrDU labeling using Fluorescein (FITC)-tagged anti-BrdU antibody (BD Biosciences, Palo Alto CA) as we described earlier (Maddala et al., 2008). Micrographs were captured using Nikon Eclipse 90i confocal laser scanning microscope. Total numbers of nuclei staining positively for BrdU in the epithelium and transitional zone of lenses from both Rap1cKO and WT mice, were counted and plotted. Values derived from 6 independent specimens (2 to 3 serial sections from each mouse head) were analyzed for determining statistical significance.

Statistical analysis

Where required, the student's t-test was performed to determine significance of differences between the Rap1cKO and WT specimens. Values are represented as Mean ± Standard Error of the Mean (SEM).

Results

Rap1 is abundantly expressed in the mouse lens and distributes predominantly to the plasma membrane

To obtain baseline information regarding the expression profile of Rap1 GTPase, its regulatory proteins including GEF and GAP, and proteins that interact with Rap1 including afadin and nectin in the ocular lens, we evaluated and confirmed the expression of Rap1a, Rap1b, RapGAP, C3G, Epac, Rap-GDP dissociation stimulator (GDS), afadin and nectin by RT-PCR analysis of both neonatal (P2) and P24 mouse lenses (Fig. 1A). Following this, we

determined the relative expression profile of Rap1a and Rap1b in neonatal mouse lenses by qRT-PCR. Interestingly, the relative levels of Rap1a and Rap1b were found to be much higher than those of the house keeping gene glyceraldehyde 3-phosphate dehydrogenase (GAPDH), refer to Fig. 1B, with the expression levels of Rap1b being significantly higher (2.75-fold) than Rap1a in neonatal lenses (n=3; $p<0.01$; Fig. 1C). In P21 mouse lenses, Rap1 (both Rap1a and Rap1b) protein was found to be distributed predominantly to the membrane-enriched fraction based on immunoblot analysis of lens soluble and membrane-enriched fractions as shown in Fig. 1D. Additionally, we examined the distribution pattern of Rap1 in E10.5 and P21 mouse eye by immunofluorescence analysis using paraffin embedded tissue sections and polyclonal Rap1 antibody which reacts with both Rap1a and Rap1b. As shown in Fig. 1E, Rap1 is distributed throughout the lens pit, and consistent with the results of immunoblot analysis (Fig. 1D), is mostly membrane associated (Fig. 1E insert) and distributed throughout the lens (P21), including epithelium (not shown in Fig.1, but can be seen in Fig.2) and fiber cells.

Conditional deficiency of Rap1 (Rap1a/Rap1b) leads to microphthalmia and lens opacification in embryonic and neonatal mice

To explore a plausible non-compensating role(s) for Rap1a and Rap1b in lens morphogenesis and architecture, we initially performed a histological examination of eyes derived from Rap1a and Rap1b adult null mice, which have been previously thoroughly characterized and confirmed to not exhibit any known ocular phenotype (Chrzanowska-Wodnicka et al., 2008; Li et al., 2007). Light microscopy analysis of paraffin embedded sagittal tissue sections derived from age-matched adult Rap1a and Rap1b null and WT mouse eyes stained with H&E did not reveal any differences in either the lens epithelium (thickness, cell shape and nuclei) or in fiber cells (shape or arrangement) indicating that Rap1a and Rap1b serve compensatory roles in the lens (data not shown).

Based on the above described observations, and given that Rap1a and Rap1b double null mice have been reported to be embryonically lethal (Chrzanowska-Wodnicka et al., 2008; Li et al., 2007), we developed a conditional Rap1a/Rap1b double knockout mouse (described hence forth as Rap1 cKO.) This mouse model was generated by crossing the well characterized Rap1a and Rap1b double floxed mice (Pan et al., 2008) with transgenic Le-Cre mice expressing Cre recombinase in a lens specific manner (Ashery-Padan et al., 2000). Recombination of the conditional Rap1a and Rap1b alleles led to a dramatic reduction (~90%) in Rap1 (both Rap1a and Rap1b) protein levels in the E17.5 mouse lens membrane-enriched fraction based on immunoblot analysis (data shown for representative 3 independent pooled lens specimens from both WT and Rap1 cKO mice; Fig. 2A &B). These results were consistent with reduced Rap1 immunofluorescence staining observed in the intact lens (both epithelium and fibers) of E17.5 Rap1 cKO mouse embryo relative to the respective WT control (Fig. 2C). Although Cre expression was confirmed in the E11.5 Rap1 cKO mouse using a Cre-activatable GFP reporter gene, immunofluorescence analysis suggest that Rap1 may not be completely absent from E11.5 Rap1 cKO lens specimens relative to WT controls (Fig. 2C). It is also plausible that the low-level immunofluorescent staining for Rap1 in these specimens derives partly from non-specific background staining.

Conditional deficiency of Rap1 led to a severe bilateral ocular phenotype including microphthalmia and lens opacification in E17.5 and PI neonatal mice (Fig. 2D, images are shown for the E17.5 specimens with eye lids removed). These ocular phenotypes were found to be consistent in almost 100% of the animals. Lens opacification in the central or nuclear region was evident in both E17.5 and P1 mice. In older Rap1 cKO mice (>P1), there was extensive degeneration of the lens with a severe microphthalmic phenotype (not shown). Due to this severe lens phenotype in Rap1 cKO mice, most of the analyses for the remainder of the study were performed using immunofluorescence analyses of embryonic specimens. Only limited immunoblotting-based protein quantification analyses were performed using E17.5 embryonic lenses extracted and pooled from Rap1 cKO mice.

Impairment of lens morphogenesis in Rap1 cKO mice

To determine the impact of Rap1 deficiency on lens morphogenesis, cacodylate buffer fixed, paraffin embedded, H&E stained sagittal sections from the Rap1 cKO embryonic (E11.5, 13.5, 15.5 and 17.5) mouse head were examined by light microscopy. Lens vesicle formation and separation in E11.5 Rap1cKO mouse ocular specimens was found to be similar to that in WT controls (Fig. 3A). In E13.5 specimens, while differentiated lens primary fibers elongated and filled the lumen of the lens vesicle similar to what was noted for WT controls, the apical ends of primary fiber cells however, did not form adhesive/junctional attachments with epithelial cell apical ends leading to an empty space between the epithelium and primary fiber cell apical tips (Figs. 3A; this can also be clearly seen in the tissue sections stained for F-actin shown in Fig. 3B). Additionally, the anterior-posterior alignment and migration pattern of primary and secondary lens fiber cells was found to be abnormal and different from those of WT controls. Instead of aligning straight with the central epithelium, the apical tips of primary fiber cells were found to be oriented either to the left or right side of the central epithelium. Moreover, the secondary lens fibers of Rap1 cKO mice exhibit a sharp bending towards the lens fulcrum (the region where the early elongating lens epithelial apical ends meet with the apical tips of newly differentiating fibers)(Sugiyama et al., 2009) and subsequently, these cells also failed to gain a typical concave shape from their initial convex shape and to maintain apical-basal polarity. In E15.5 Rap1 cKO lens specimens, there is a wide gap between the fiber cell apical ends and epithelium indicating impaired formation of apical junctions between the apical ends of epithelial cells and fiber cells compared to the WT controls. Additionally, in E15.5 Rap1 cKO lens specimens, there is an abnormal distribution pattern of nuclei and thickening of transition zone extending towards posterior region compared to the WT controls. The nuclei are distributed below to the bow region, being retained at the basal tips of the fiber cells. In E17.5 and P1 Rap1 cKO lenses, there is a gross and progressive disruption in the apical junctions between the lens epithelium and fiber cell apical tips. In contrast, the Rap1 cKO mouse lens specimens derived from the E13.5 to P1 stages showed no obvious abnormalities in cell adhesion between the fiber cell basal ends and the inner surface of the posterior capsule which is made up of basement membrane matrix.

In addition to the histological changes described above based on H&E staining, we stained the same stages of embryonic lenses (cryofixed) for F-actin using rhodamine-phalloidin (red staining). The nuclei are stained in these specimens using Hoechst (blue). Consistent with

the H&E based histological changes, the F-actin stained lens specimens derived from the Rap1 cKO mice showed defects in apical cell junctional interactions between the epithelium and fiber cells (indicated with arrows), fiber cell migration pattern and apical to basal cell polarity. In these actin stained specimens, it was noticeable that the newly forming secondary fibers fail to form apical junctions with early elongating epithelium leading to disrupted formation of the lens fulcrum in the Rap1 cKO mouse specimens compared with WT controls (indicated with arrow heads in Fig. 3B.) With respect to F-actin organization, there was a noticeable reduction in F-actin staining at the apical ends and intercellular junctions of the lens vesicle in E11.5 specimens, and apical junctions of epithelial and fiber cells in E13.5–E17.5 specimens derived from the Rap1 cKO mouse embryos compared with the WT controls. Compared to Rap1 cKO mice, Le-Cre specimens did not exhibit any noticeable lens or ocular phenotype relative to WT specimens (data not shown).

Rap1 deficiency suppresses formation of adherens junctions (AJs) and ZO-1 based cell-cell interactions in mouse lens

The Rap1 cKO mouse lens epithelium exhibited progressive morphological changes (central and equatorial) starting from E13.5, with significant decrease (> 40%) in epithelial width (apical to basal length; Fig. 4A4) and alterations in epithelial cell shape in E15.5 and E17.5 specimens, relative to WT controls (Fig. 4A1–3). Moreover, a dramatic and progressive loss was also observed in E-cadherin –based cell-cell junctions in the lens epithelium (both in central and equatorial) starting from E13.5 to E17.5 in the Rap1 cKO mouse embryos, indicating disruption of AJs (Fig.4A 2&3). The disruption of E-cadherin-based cell junctions was found to affect epithelial cell shape, resulting mainly in size reduction and shape change from an elongated columnar to a stunted profile.

In addition to the AJs, we also evaluated the integrity/formation of ZO-1 based cell-cell interactions in Rap1 cKO lenses of E13.5 to E17.5 mouse embryos by immunofluorescence labeling of ZO-1. As has been reported previously (Pontoriero et al., 2009), ZO-1 was localized at the interface of apical ends of lens epithelial and fiber cells (Fig. 4B). At E13.5 in WT lens specimens, ZO-1 was distributed discretely at the apical junctions of epithelium and primary fiber cells (indicated with arrows in Fig. 4B). Subsequently in E15.5 and E17.5 WT lens specimens, the ZO-1 staining distributes intensely at the lens fulcrum region (Fig. 4, arrows), in agreement with previous reports (Pontoriero et al., 2009; Sugiyama et al., 2009). However, the ZO-1-based cell-cell junctions were almost completely absent in the Rap1 cKO lenses compared with WT controls (Fig. 4B). As can be seen in Fig. 4B, in the Rap1 cKO mouse epithelium, the size and number of nuclei is also reduced dramatically based on Hoechst staining (blue) compared with WT controls.

Consistent with loss of E-cadherin based AJs, β-catenin distribution (based on immunofluorescence labeling) at the AJs was also dramatically and progressively reduced in the Rap1 cKO mouse lens epithelium of E13.5 to E17.5 specimens relative to WT controls (Fig. 5A). The loss of β-catenin based AJs in Rap1 cKO lens specimens was also found to be associated with altered epithelial cell shape as shown in Fig. 4 (Fig. 5A, see inserts). Collectively, the changes observed in E-cadherin and β-catenin distribution suggest that absence of Rap1 results in impaired AJ formation in the lens epithelium (Fig. 4 & 5). Unlike

E-cadherin, the distribution of which is lens epithelium specific (Leong et al., 2000; Pontoriero et al., 2009), N-cadherin distributes to both the lens epithelium and fibers cells, exhibiting a much higher staining intensity in fiber cells relative to the epithelium as shown in Fig. 5B. Interestingly, N-cadherin distribution in the lens epithelium increased progressively and robustly in Rap1 cKO mouse embryos starting from E 13.5 to E17.5 and was comparable to that noted in WT controls, as assessed by immunofluorescence analysis (Fig. 5B, see the inserts). In contrast, N-cadherin distribution in fiber cells of Rap1 cKO mouse lens appears to be reduced but not dramatically relative to fiber cells from WT control lenses. Le-Cre lens specimens derived from both E15.5 and 17.5 embryonic mice did not exhibit noticeable changes either in E-cadherin-based AJs and ZO-1 based cell-cell junctions compared to WT specimens (data not shown).

Rap1 deficiency disrupts cell-matrix adhesion, β1-integrin activation and PAR complex in mouse lens

Since Rap1 is known to regulate cell-extracellular matrix (ECM)-based cell adhesive interactions through Krit1, RIAM, talin and integrins (Bos et al., 2003; Kim et al., 2011; Lee et al., 2009), we evaluated the status of these interactions in Rap1 cKO mouse lenses by measuring changes in paxillin phosphorylation and β1 integrin activation using immunofluorescence analysis. Paxillin is a well characterized multi-domain adaptor protein known to interact with integrins and vinculin in a phosphorylation-dependent manner at the focal adhesions (Turner, 2000). Phosphorylation of paxillin at Tyr118 is mediated by focal adhesion kinase (Turner, 2000). Using a Tyr118 specific phospho-paxillin antibody, we examined the distribution profiles of phosphorylated paxillin in Rap1 cKO mouse lenses by immunofluorescence analysis of tissue cryosections. In WT lens specimens derived from both E15.5 and E17.5 mouse embryos, phospho-paxillin staining localized discretely and intensely at the apical junctions of primary lens fibers and epithelial cells, similar to the distribution pattern of ZO-1, as shown in Fig. 6A (arrows). There was also some phospho-paxillin staining throughput the lens capsule, however it is not presently clear whether this staining is specifically attributable to the basal tips of epithelial and fiber cells. However, in E15.5 and E17.5 Rap1 cKO mouse lens specimens, there was an almost complete loss of phospho-paxillin staining at the apical junctions of epithelial and fiber cells as shown in Fix. 6A. We then examined for changes in β1 integrin by immunofluorescence analysis, using a monoclonal antibody (9EG7) which recognizes an activated epitope of β1 integrin in zinc fixed, paraffin embedded lens sections. In WT specimens, weak immunostaining for β1 integrin was found to be distributed throughout the lens, including epithelium and fibers (in red). Intriguingly, in Rap1 cKO specimens, particularly those derived from the E17.5 embryos, we noted a robust increase of immunostaining for β1 integrin in the lens epithelium compared to the corresponding WT controls (Fig. 6B, indicated with arrows). This change in β1 integrin (total as well as activated) was found to be more intense in the central epithelium relative to the equatorial epithelium (Fig. 6B). Collectively, the changes recorded in phospho-paxillin and β1 integrin in the Rap1 cKO mouse lens specimens indicate dysregulated cell-ECM interactions in the absence of Rap1.

Based on the changes involving apical junctions, epithelial cell shape, disruptions in ZO-1 based cell-cell junctions, AJ and loss of apical to basal alignment of fiber cells in Rap1 cKO

lenses, we asked whether regulatory mechanisms governing cell polarity are perturbed in the deficiency of Rap1 from the lens. Indeed Rap1 activity has been shown to be required for activation of the PAR (Partitioning-defective) protein complex controlling cell polarity (Baum and Georgiou, 2011; Gerard et al., 2007; Lampugnani et al., 2010). Moreover, some of the abnormalities of Rap1 cKO mouse lens including defective lens fulcrum formation and apical junctions at fulcrum were found to be very similar to the changes reported in the aPKCλ deficient mouse lens (Sugiyama et al., 2009). aPKC (including aPKCλ and aPKCς) has been characterized as a critical components of the PAR protein complex consisting of PAR3, PAR6, Cdc42 and aPKC (Etienne-Manneville and Hall, 2003; Suzuki and Ohno, 2006). Therefore, we explored whether there were detectable changes in the levels of aPKCλ and aPKCς in the E17.5 Rap1 cKO lens (in 800×g total protein fractions) by immunoblotting analysis. We found a significant decrease in the levels of both aPKCλ and aPKCς in Rap1 cKO lenses relative to WT controls, with the changes being much more pronounced in the case of aPKCς (Fig. 6C). Both forms of aPKC were noted to be distributed throughout WT lens as assessed by immunofluorescence profiles (not shown).

Induction of EMT in the Rap1 deficient mouse lenses

Since Rap1 cKO mouse lenses exhibited a dramatic disruption in E-cadherin based AJs and ZO-1 based cell-cell interactions, we asked ourselves whether epithelial plasticity and characteristics are altered under these conditions, and assessed for changes in expression of αSMA, commonly considered a biomarker of EMT (epithelial to mesenchymal transition) (Kalluri and Neilson, 2003; Kalluri and Weinberg, 2009). To this end, cryosections from Rap1 cKO lenses derived from E13.5, E15.5 and E17.5 mouse embryos were immunostained with a monoclonal antibody to αSMA conjugated with Cy3. Presumptive tissues of the iris and ciliary body, but not lens tissue, were found to exhibit αSMA-specific positive staining in E15.5 and E17.5 ocular specimens from WT animals (Fig. 7A). By contrast, in Rap1 cKO mouse specimens, the lens epithelium starting from E13.5 exhibited progressively increased αSMA specific staining (Fig. 7A, arrows). In E17.5 Rap1 cKO mouse specimens, the distribution of αSMA staining in lens epithelium was localized intensely to the cell-cell junctions (Fig. 7A, arrows). In contrast to the Rap1 cKO mouse specimens, Le-Cre lenses (E15.5 and 17.5) did not exhibit presence of αSMA (data not shown). The results from distribution analysis of αSMA together with the loss of E-cadherin-based AJs and ZO-1 based cell-cell interactions, and increased N-cadherin observed in lens epithelium of Rap1 cKO mouse point to altered lens epithelial plasticity and induction of EMT. Based on these observations, we also evaluated the distribution of vimentin, an intermediate filament cytoskeletal protein and a known marker of EMT (Kalluri and Neilson, 2003), in E17.5 Rap1 cKO mouse lenses by immunofluorescence analysis of cryofixed tissue sections. As shown in Fig. 7B, in WT specimens, lens fibers stain intensely for vimentin with only weak staining observed in the epithelium. In Rap1 cKO specimens the staining profile for vimentin appears to be reversed, where increased vimentin immunostaining is associated with the lens epithelium (Fig. 7B, inserts, arrows), accompanied by a marked decrease of vimentin staining in the lens fibers, relative to the staining profiles noted for WT controls (Fig. 7B).

Robust upregulation of expression of E-cadherin suppressing transcription factors and Dihydropyrimidine dehydrogenase in the Rap1 cKO mouse lens

Our observations of disrupted AJs and ZO-1 based cell-cell interactions, concomitant with increases in immunostaining for αSMA, vimentin and N-cadherin, are indicative of induction of EMT in the lens epithelium of the Rap1 cKO mouse (Kalluri and Weinberg, 2009; Thiery et al., 2009). To gain insights into the molecular mechanisms involved in initiation of EMT and loss of E-cadherin based AJs in Rap1 cKO mouse lens, we explored for changes in the expression of Snai1, Slug, Zeb1 and Zeb2, which are well-characterized transcriptional suppressors of E-cadherin (Puisieux et al., 2014). Additionally, we conducted qRT-PCR analysis of E17.5 Rap1 cKO mouse lenses to determine expression profile of the metabolic enzyme dihydropyrimidine dehydrogenase (DYPD), which has been demonstrated to play an essential role in EMT by regulating the levels of dihydropyrimidines (Shaul et al., 2014). For these analyses, total RNA was extracted from pooled intact lenses (E17.5), and three pooled samples from WT and Rap1 cKO analyzed for comparison. Expression of Snai1, Slug, Zeb2 and DYPD was significantly and robustly increased in E17.5 Rap1 cKO mouse lenses compared to the WT controls (Fig.8A). Unlike Zeb2, Zeb1 expression was not significantly altered in Rap1 cKO mouse lenses (Fig. 8A). Analysis of Slug protein levels and distribution profile using immunofluorescence analysis of paraffin embedded ocular specimens from Rap1 cKO and WT mouse embryos, by E15.5 and E17.5 revealed that Slug distribution in the Rap1 cKO mouse lens epithelium increased starting from E15.5, being robustly increased in E17.5 specimens relative to WT controls, as shown in Figure 8B. A slight increase of Slug was also evident in lens fiber cells of Rap1 cKO mice relative to the WT control (Fig. 8B).

Rap1 deficiency affects cell proliferation and survival in mouse lens

The Rap1 deficient mice generated in our study exhibited micropthalmia and smaller lenses (Fig. 2) leading to the conclusion that Rap1 might potentially influence cell cycle progression and proliferation in the Rap1 cKO mouse lenses. To explore this possibility, we assessed lens proliferation status using *in vivo* BrdU incorporation in E15.5 embryos. These experiments were performed by injecting pregnant mice with BrdU as described in the Methods section. Embryonic head cryosections immunolabelled for BrdU using FITC-conjugated BrdU monoclonal antibody were scored for BrdU positive cells (green/yellow stain) in the different regions of lens epithelium including central epithelium and transitional zone. In WT E15.5 lenses, BrdU incorporation was found to be intense and exclusively located in the epithelium, with no incorporation detected in the transitional zone (Fig. 9A, see arrows). In Rap1 cKO mouse lenses, there is a significant decrease (>60%) in BrdU positive cells in the epithelium above the transitional zone based on the values derived from 6 independent specimens (Fig. 9A). Interestingly however, there was a significant increase in BrdU positive cells in the transitional zone of Rap1 cKO lens specimens (indicated with arrows in Fig. 9A) compared to WT controls, indicating a failure of epithelial cells to exit from cell cycle progression at the transitional zone. Additionally, and unlike the case in WT specimens, the distribution of nuclei (propidium iodide positive red stain) in fiber cells of Rap1 cKO specimens shifts to below the bow region, localizing to the posterior or basal

ends of fiber cells (Fig. 9A, see arrow heads), presenting a distribution pattern very similar to that commonly seen in the epithelium at the anterior part of lens (Fig. 9A).

To determine the cell survival status in the absence of Rap1 in lens, cryofixed head tissue specimens derived from E15.5 and E17.5 WT and Rap1 cKO mouse embryos were labelled for apoptotic cells by TUNEL staining using an ApopTag Plus Fluorescein kit. TUNEL positive cells (green/yellow) were counted in lens epithelium and fibers. Based on values (mean ±SEM) derived from 6 independent specimens, TUNEL positive cells were significantly increased in the epithelium and fiber cells of Rap1 cKO mouse lenses (both E15.5 and E17.5) compared to the respective WT controls (Fig. 9B). TUNEL positive cells increased progressively with a much higher number being observed in E17.5 relative to E15.5 specimens from Rap1 cKO mice (Fig. 9B). These observations reveal increased apoptotic cell death in the Rap1 deficient mouse lenses.

Rap1 deficiency does not impair lens fiber differentiation

Fiber cell differentiation is one of the major cellular processes of lens morphogenesis and the fiber cells make up the bulk of the lens mass(Cvekl and Ashery-Padan, 2014). Epithelial cells at transitional zone of lens exit from cell cycle, elongate and differentiate into ribbon like fiber cells. These differentiating fibers express several fiber cell specific proteins including aquaporin-0, crystallins (β and γ) and beaded filament proteins-phakinin and filensin(Cvekl and Ashery-Padan, 2014). To evaluate whether the absence of Rap1 affects lens fiber cell differentiation, we examined the distribution pattern of aquaporin-0, a water channel protein and γ-crystallin using immunofluorescence analysis of cryofixed tissue specimens. As shown in Fig. 10, E17.5 Rap1 cKO lens specimens exhibit a typical fiber cell elongation pattern and expression of fiber cell specific differentiation markers including aquaporin-0 and γ-crystallin, similar to the findings noted in WT controls, indicating normal lens differentiation in the deficiency of Rap1. Interestingly, in some specimens, the apical surface of lens epithelium in E17.5 Rap1 cKO mouse stained positively for aquaporin-0 based on immunofluorescence compared to WT (Fig. 10, see arrow), indicating a possible mixed epithelial/fiber cell phenotype.

Discussion

The broad objective of our study was to explore the role of Rap1 GTPase in vertebrate lens development and architecture. Our results provide genetic evidence for the requirement of Rap1 GTPase in controlling mouse lens organ morphogenesis. Importantly this study reveals impaired epithelial cell AJs, ZO-1 associated cell junctions and polarity in the absence of Rap1 GTPase (Rap1a and Rap1b) leading to defects in lens morphogenesis and integrity in a mouse model, thereby demonstrating the requirement for Rap1 in regulation and establishment of cell adhesive interactions and cell polarity, and epithelial organ formation and architecture. Moreover, our study also illuminates that the defects in lens epithelial cell-cell junctions, cell shape and polarity in Rap1 deficient lenses are associated with induction of epithelial plasticity and acquisition of mesenchymal characteristics by epithelial cells, as evidenced by increases in expression of E-cadherin suppressing transcription factors and DYPD in lens epithelial cells. These observations offer important molecular insights into

EMT and fibrosis, a common cause for metastatic cancers, fibrotic diseases and for secondary cataract formation in human patients (Eldred et al., 2011; Kalluri and Weinberg, 2009; Thiery et al., 2009).

Rap1 regulated establishment of epithelial cell-cell junctions, cell-matrix interactions and cell polarity is considered to be critical not only for cell migration, proliferation, differentiation and survival but also for organ development and tissue architecture (Asha et al., 1999; Boettner and Van Aelst, 2007; Boettner and Van Aelst, 2009; Choi et al., 2013; Kooistra et al., 2007; O'Keefe et al., 2012; Spahn et al., 2012). However, the presumed role(s) of Rap1 in vertebrate organ development and integrity has remained unproven. To the best of our knowledge this is the first study addressing this aspect of Rap1 function. Rap1 is an evolutionarily conserved protein and is widely expressed in different tissues (Kooistra et al., 2007). Rap1 (both Rap1a and Rap1b) is distributed in both the developing and mature mouse lens, including the lens vesicle, epithelium and fibers, localizing predominantly to the cell-cell junctions and membrane. Although Rap1a and Rap1b, which are 95% identical by amino acid sequence encoded by two different genes (Noda, 1993) have been shown to have some non-redundant roles in angiogenesis, vascular endothelial cells and other cell types (Chrzanowska-Wodnicka, 2013), adult Rap1a or Rap1b null mice do not reveal any overt lens defects indicating that these proteins have compensatory role(s) in the lens.

Contrastingly, the Rap1a and Rap1b double conditional knock-out (cKO) mice developed in this study exhibited lens defects starting from E13.5, and the gross lens defects and opacification observed in E17.5 mouse embryos reveal a requirement for Rap1 in lens morphogenesis and integrity. The Le-Cre transgenic mice used in this study express Cre recombinase in the presumptive lens ectoderm prior to lens vesicle formation (Ashery-Padan et al., 2000). In E11.5 Rap1 cKO mouse lenses, although Cre recombinase was robustly expressed, Rap1 expression appears to be not completely abolished based on immunofluorescence and the lens vesicle was noted to exhibit normal formation and separation. Since we have not confirmed complete absence of Rap1 in E11.5 Rap1 cKO lenses by direct methods such as immunoblot analysis, we cannot definitively conclude that Rap1 plays an indispensable role in lens early development. Differentiation of lens primary fiber cells was found to be normal in E13.5 Rap1 cKO mouse embryos. Defects were evident however in the apical tip attachments between lens primary fiber cells and epithelial cells of E13.5 and E15.5 Rap1 cKO mice. These defects result in a clear gap between the epithelium and fiber cell apical tips, demonstrating impaired formation of apical junctions in the absence of Rap1 during lens morphogenesis. Additionally, lens fulcrum formation was impaired due to defective apical-apical junctions between the overlying early elongating epithelial cells and newly forming secondary fibers in developing (E13.5 and E15.5) Rap1cKO mouse lenses. This observation of an abnormal lens fulcrum phenotype in the Rap1 cKO mouse overlaps with that reported previously in the aPKCλ deficient mouse lens(Sugiyama et al., 2009). aPKCλ and the related aPKCς are critical components of the PAR complex required for normal polarization of epithelial cells (Choi et al., 2013; Humbert et al., 2006; Suzuki and Ohno, 2006). The decreased levels of aPKCλ and aPKCς observed in the Rap1 cKO mouse lenses are indicative of compromised apical junctional polarity in both epithelial and fiber cells. Primary fiber cells exhibit apical to basal alignment by

forming adhesive interactions involving the apical ends of epithelial and primary fibers at the anterior end, and between the basal ends of primary fibers and basement membrane of the posterior capsule at the posterior end. Lens primary fiber cells from the Rap1 cKO mice exhibited noticeable abnormalities primarily in their anterior alignment with epithelial cells while maintaining normal alignment at posterior. Additionally, the lens secondary fibers from Rap1 cKO mice exhibit a dramatic curvature towards the lens fulcrum indicating an abnormal migration pattern. Collectively, these observations reveal defects in fiber cell adhesion and migration events together with impairments in establishment of epithelial and fiber cell polarity in the Rap1 cKO mouse lens. Consistent with these observations, Rap1 along with its effector molecule Canoe/afadin has been demonstrated to regulate apical-basal cell polarity in Drosophila, and requirement of PAR complex activation in Rap1 regulated polarity in immune cells (Boettner and Van Aelst, 2007; Boettner and Van Aelst, 2009; Gerard et al., 2007; Lampugnani et al., 2010; O'Keefe et al., 2012; Sawyer et al., 2009; Spahn et al., 2012).

In Rap1 cKO mouse lenses, one of the earliest and easily detectable phenotypes we noted was epithelial thickness and cell shape changes. The thinning of epithelium and shortened epithelial cell width was clearly evident in Rap1 cKO lenses starting from E13.5 to E17.5, relative to the striking apical-basal columnar cell shape noted in normal mouse lenses, revealing the disruption of epithelial cell shape and polarity in the absence of Rap1. Importantly, these changes were found to be closely associated with a marked and progressive reduction in E-cadherin and β-catenin-based AJs and ZO-1-based cell-cell interactions in the Rap1 cKO mouse lens epithelium. These observations are consistent with the well-documented characteristics of Rap1 GTPase in cultured epithelial cells of different tissues and in epithelial morphogenesis in Drosophila (Asha et al., 1999; Boettner and Van Aelst, 2007; Boettner and Van Aelst, 2009; Knox and Brown, 2002; Kooistra et al., 2007; Sawyer et al., 2009; Spahn et al., 2012). Interestingly, in contrast to E-cadherin, N-cadherin-showed a robust and progressive increase in the lens epithelium of Rap1 cKO mice between E15.5 and E17.5. Although Rap1 has been shown to regulate N-cadherin-based AJs and polarity in neuronal cells (Jossin and Cooper, 2011), the upregulation of N-cadherin in the lens epithelium of Rap1 cKO mice could be a secondary response to the altered epithelial plasticity and EMT noted in these lenses since elevated levels of collagen in cells undergoing EMT have been shown to upregulate N-cadherin (Shintani et al., 2008). The loss of ZO-1 based cell adhesive interactions observed in Rap1 deficient lenses in this study support earlier observations reported in cultured epithelial cells and in Drosophila lacking Rap1 and its effector molecule afadin (Choi et al., 2011; Mandai et al., 2013; Mandell et al., 2005; Ooshio et al., 2010; Pannekoek et al., 2009). These changes could be also arising in part from impaired formation of AJs, because conditional deletion of E-cadherin has been shown to impair formation of ZO-1-based cell-cell junctions in the mouse lens epithelium (Pontoriero et al., 2009). Similarly, absence of aPKCλ and Scrub(Sugiyama et al., 2009; Yamben et al., 2013), which are well characterized regulators of cell polarity in the lens, has been shown to disrupt ZO-1 based cell adhesive interactions of epithelium providing further support for the importance of Rap1 in maintaining lens epithelial polarity and cell adhesive interactions. Although we have not examined cytoskeletal protein organization especially myosin II at the AJs in the Rap1 cKO mouse epithelium, it is likely a disruption in actin and

myosin II – based cytoskeletal organization underlies the impaired formation and stability of AJs noted in the Rap1 deficient lenses. We did, however, find a marked decrease in Rac1 GTPase protein in both epithelium and fibers of Rap1 cKO mouse embryonic lens, relative to the WT control (data not shown), and Rac1 has been demonstrated to act downstream to Rap1 and regulate AJs, cytoskeletal organization and cell migration (Fukuyama et al., 2006; Maddala et al., 2011a; Rikitake et al., 2012).

Rap1 cKO mouse lenses also exhibited disruption of cell-matrix adhesive interactions based on the decreased phospho-paxillin at apical junctions of epithelium and primary fibers noted in our study. Focal adhesion kinase (FAK) regulated phosphorylation of the Tyr 118 residue of paxillin plays a critical role in fibronectin assembly and cell-ECM interactions (Turner, 2000). FAK, integrin-α5 and fibronectin-1 have been shown to be required for lens fiber cell morphogenesis in zebrafish (Hayes et al., 2012). Interestingly, the distribution pattern of phospho-paxillin at the apical junctions of mouse lens epithelium noted in this study appears to be identical to that reported for fibronectin in the zebrafish lens (Hayes et al., 2012). Therefore, maintenance of paxillin-based cell adhesive interactions at the apical junctions of lens epithelium regulated by Rap1 appears to be critical for lens morphogenesis. Intriguingly, although Rap1 has been demonstrated to regulate integrin-mediated cell adhesive interactions through RAIM, Krit and Talin, and to be involved in the Rap1GAP-mediated inactivation of β1-integrin (Kim et al., 2011; Potla et al., 2014), we found increased levels of immunostaining for β1-integrin in the epithelium of Rap1 deficient lenses. This increase in β1-integrin staining which might indicate a possible increase in both, activation and protein expression was particularly noticeable at E17.5 at which stage the Rap1 cKO associated ocular phenotype is severe. Whether this is a secondary response to the dramatic impairment observed in cell junctional and cell adhesive interactions in the Rap1 cKO mouse lens is not clear at this point. Taken together the observation of reduced phospho-paxillin and deregulated β1-integrin activation and expression in the Rap1 cKO lenses indicate dysregulated cell-matrix interactions in Rap1 deficiency.

Another major phenotypic feature associated with the deficiency of Rap1 was epithelial to mesenchymal transition (EMT) in the lens epithelium, as inferred from the marked induction of α-smooth muscle actin (αSMA), along with vimentin and N-cadherin noted in the lens epithelium, concomitant with loss of AJs in E15.5 and E17.5 Rap1 cKO mice, suggestive of an alteration in epithelial plasticity with epithelial cells transitioning into a mesenchymal phenotype (EMT). We also obtained additional evidence in support of EMT in Rap1 cKO mouse epithelium as inferred from the induction of expression of dihydropyrimidine dehydrogenase (DYPD). DYPD has been identified as a mesenchymal metabolic signature and dihydropyrimidine generated by DYPD has been shown to be essential in initiation of EMT in various cancer cell lines (Shaul et al., 2014). Furthermore, consistent with loss of AJs, our results on upregulation of E-cadherin suppressing transcription factors including Snai1, Slug and Zeb2 in Rap1 cKO mouse lens epithelium also support the occurrence of EMT events in these lenses. These multiple molecular changes induced in the deficiency of Rap1 in lens epithelium represent the common characteristics of EMT (Kalluri and Neilson, 2003; Kalluri and Weinberg, 2009; Puisieux et al., 2014; Thiery et al., 2009). One exception to this conclusion is Zeb2, the absence of which has been reported to not have significant impact on mouse lens epithelial phenotype (Manthey et al., 2014). Recently Scrib deficiency

induced EMT in lens epithelium has also been reported to be associated with elevated levels of Snai1 in mouse lens (Yamben et al., 2013), similar to the findings of this study in the absence of Rap1. Moreover, previous reports on the induction of EMT in the lens epithelium in association with loss/disruption of AJs in the absence of E-cadherin (Pontoriero et al., 2009), aPKCλ (Sugiyama et al., 2009) and Scrub (Yamben et al., 2013) are consistent with the Rap1 deficiency-mediated changes observed in this study. Although EMT has a fundamental role in early developmental processes and wound healing (Nieto, 2013; Thiery et al., 2009), dysregulated EMT can lead to fibrosis, metastasis and other fibrotic complications including posterior capsular cataracts(Eldred et al., 2011; Kalluri and Weinberg, 2009; Mamuya et al., 2014; Menko et al., 2014; Stump et al., 2006; Thiery et al., 2009). Therefore, our observation on Rap1 deficiency-induced EMT uncovers the importance of Rap1 in controlling epithelial phenotype and EMT in different tissues.

Finally, the smaller lenses and microphthalmic eye phenotypes observed in the deficiency of Rap1 in association with increased apoptosis of lens epithelial and fiber cells point to compromised cell survival as the basis for observed changes in lens size and eye size in the absence of Rap1. This is also consistent with previous observations of increased programmed cell death in conjunction with loss or disrupted cell-cell junctions in the absence of E-cadherin and N-cadherin in the mouse lens (Pontoriero et al., 2009). Rap1 is also expected to influence cell survival through other mechanisms such as regulation of various MAP kinases (Raaijmakers and Bos, 2009). Additionally, our results from in vivo BrdU labelling experiments indicate that Rap1 deficiency leads to impaired cell cycle progression especially in the central epithelial cells of E13.5 and E15.5 mouse lenses indicating decreased cell proliferation in this region. The observation of increased BrdU incorporation at the transitional zone in the Rap1 cKO mouse lens, however, which is suggestive of defective cell cycle exit, could be related partly to the defects in cell polarity and apical junction formation discussed earlier, wherein the inability of early elongating epithelial cells to form apical cell-cell junctions with newly forming fibers results in marked disruption of lens fulcrum formation (Sugiyama et al., 2009). Rap1 deficiency appears to have no overt impact on lens fiber cell differentiation based on the normal expression of differentiation markers in Rap1 deficient lenses, indicating that alterations of cell adhesive interactions and polarity may not be critical for Rap1-regulated fiber cell differentiation. In conclusion, this study provides unequivocal genetic evidence for the requirement of Rap1 GTPase in controlling mouse lens organ morphogenesis by regulating and maintaining epithelial cell-cell junctions, cell-matrix interactions, polarity and survival.

Supplementary Material

Refer to Web version on PubMed Central for supplementary material.

Acknowledgments

We thank Magdalens Chrzanowska-Wodnicka, Lawrence Quilliam and Ashery-Padan for their generous help in providing the Rap1a null mouse eyes, Rap1b null mouse eyes and the Le-Cre transgenic mice, respectively. We also thank Sam Zigler, Jr, Roy Quinlin and Joe Horwitz for providing the γ-crystallin, vimentin and aquaporin-0 antibodies, respectively. This work was supported by the National Institutes of Health grants to P.V. Rao (EY025096 and EY018590), R.A. Lang (EY17848), and by a National Eye Institute Core Grant for Vision Research (P30-EY5722).

References

Ando K, Fukuhara S, Moriya T, Obara Y, Nakahata N, Mochizuki N. Rap1 potentiates endothelial cell junctions by spatially controlling myosin II activity and actin organization. J Cell Biol. 2013; 202:901–16.

Arthur WT, Quilliam LA, Cooper JA. Rap1 promotes cell spreading by localizing Rac guanine nucleotide exchange factors. J Cell Biol. 2004; 167:111–22.

Asha H, de Ruiter ND, Wang MG, Hariharan IK. The Rap1 GTPase functions as a regulator of morphogenesis in vivo. EMBO J. 1999; 18:605–15. [PubMed: 9927420]

Ashery-Padan R, Marquardt T, Zhou X, Gruss P. Pax6 activity in the lens primordium is required for lens formation and for correct placement of a single retina in the eye. Genes Dev. 2000; 14:2701–11. [PubMed: 11069887]

Baum B, Georgiou M. Dynamics of adherens junctions in epithelial establishment, maintenance, and remodeling. J Cell Biol. 2011; 192:907–17. [PubMed: 21422226]

Boettner B, Govek EE, Cross J, Van Aelst L. The junctional multidomain protein AF-6 is a binding partner of the Rap1A GTPase and associates with the actin cytoskeletal regulator profilin. Proc Natl Acad Sci U S A. 2000; 97:9064–9. [PubMed: 10922060]

Boettner B, Van Aelst L. The Rap GTPase activator Drosophila PDZ-GEF regulates cell shape in epithelial migration and morphogenesis. Mol Cell Biol. 2007; 27:7966–80. [PubMed: 17846121]

Boettner B, Van Aelst L. Control of cell adhesion dynamics by Rap1 signaling. Curr Opin Cell Biol. 2009; 21:684–93. [PubMed: 19615876]

Bos JL, de Bruyn K, Enserink J, Kuiperij B, Rangarajan S, Rehmann H, Riedl J, de Rooij J, van Mansfeld F, Zwartkruis F. The role of Rap1 in integrin-mediated cell adhesion. Biochem Soc Trans. 2003; 31:83–6. [PubMed: 12546659]

Bulgakova NA, Klapholz B, Brown NH. Cell adhesion in Drosophila: versatility of cadherin and integrin complexes during development. Curr Opin Cell Biol. 2012; 24:702–12. [PubMed: 22938782]

Chauhan BK, Lou M, Zheng Y, Lang RA. Balanced Rac1 and RhoA activities regulate cell shape and drive invagination morphogenesis in epithelia. Proc Natl Acad Sci U S A. 2011; 108:18289–94. [PubMed: 22021442]

Choi W, Harris NJ, Sumigray KD, Peifer M. Rap1 and Canoe/afadin are essential for establishment of apical-basal polarity in the Drosophila embryo. Mol Biol Cell. 2013; 24:945–63. [PubMed: 23363604]

Choi W, Jung KC, Nelson KS, Bhat MA, Beitel GJ, Peifer M, Fanning AS. The single Drosophila ZO-1 protein Polychaetoid regulates embryonic morphogenesis in coordination with Canoe/afadin and Enabled. Mol Biol Cell. 2011; 22:2010–30. [PubMed: 21508316]

Chow RL, Lang RA. Early eye development in vertebrates. Annu Rev Cell Dev Biol. 2001; 17:255–96. [PubMed: 11687490]

Chrzanowska-Wodnicka M. Distinct functions for Rap1 signaling in vascular morphogenesis and dysfunction. Exp Cell Res. 2013; 319:2350–9. [PubMed: 23911990]

Chrzanowska-Wodnicka M, Kraus AE, Gale D, White GC 2nd, Vansluys J. Defective angiogenesis, endothelial migration, proliferation, and MAPK signaling in Rap1b-deficient mice. Blood. 2008; 111:2647–56. [PubMed: 17993608]

Cvekl A, Ashery-Padan R. The cellular and molecular mechanisms of vertebrate lens development. Development. 2014; 141:4432–47. [PubMed: 25406393]

DeMali KA, Wennerberg K, Burridge K. Integrin signaling to the actin cytoskeleton. Curr Opin Cell Biol. 2003; 15:572–82. [PubMed: 14519392]

Eldred JA, Dawes LJ, Wormstone IM. The lens as a model for fibrotic disease. Philos Trans R Soc Lond B Biol Sci. 2011; 366:1301–19. [PubMed: 21402588]

Etienne-Manneville S, Hall A. Cell polarity: Par6, aPKC and cytoskeletal crosstalk. Curr Opin Cell Biol. 2003; 15:67–72. [PubMed: 12517706]

Franke WW. Discovering the molecular components of intercellular junctions–a historical view. Cold Spring Harb Perspect Biol. 2009; 1:a003061. [PubMed: 20066111]

Frische EW, Zwartkruis FJ. Rap1, a mercenary among the Ras-like GTPases. Dev Biol. 2010; 340:1–9. [PubMed: 20060392]

Fukuyama T, Ogita H, Kawakatsu T, Inagaki M, Takai Y. Activation of Rac by cadherin through the c-Src-Rap1-phosphatidylinositol 3-kinase-Vav2 pathway. Oncogene. 2006; 25:8–19. [PubMed: 16170364]

Gerard A, Mertens AE, van der Kammen RA, Collard JG. The Par polarity complex regulates Rap1- and chemokine-induced T cell polarization. J Cell Biol. 2007; 176:863–75. [PubMed: 17353362]

Glading A, Han J, Stockton RA, Ginsberg MH. KRIT-1/CCM1 is a Rap1 effector that regulates endothelial cell cell junctions. J Cell Biol. 2007; 179:247–54. [PubMed: 17954608]

Gloerich M, Bos JL. Regulating Rap small G-proteins in time and space. Trends Cell Biol. 2011; 21:615–23. [PubMed: 21820312]

Halbleib JM, Nelson WJ. Cadherins in development: cell adhesion, sorting, and tissue morphogenesis. Genes Dev. 2006; 20:3199–214. [PubMed: 17158740]

Hayes JM, Hartsock A, Clark BS, Napier HR, Link BA, Gross JM. Integrin alpha5/fibronectin1 and focal adhesion kinase are required for lens fiber morphogenesis in zebrafish. Mol Biol Cell. 2012; 23:4725–38. [PubMed: 23097490]

Hogan C, Serpente N, Cogram P, Hosking CR, Bialucha CU, Feller SM, Braga VM, Birchmeier W, Fujita Y. Rap1 regulates the formation of E-cadherin-based cell-cell contacts. Mol Cell Biol. 2004; 24:6690–700. [PubMed: 15254236]

Humbert PO, Dow LE, Russell SM. The Scribble and Par complexes in polarity and migration: friends or foes? Trends Cell Biol. 2006; 16:622–30. [PubMed: 17067797]

Jeon TJ, Lee DJ, Merlot S, Weeks G, Firtel RA. Rap1 controls cell adhesion and cell motility through the regulation of myosin II. J Cell Biol. 2007; 176:1021–33. [PubMed: 17371831]

Jossin Y, Cooper JA. Reelin, Rap1 and N-cadherin orient the migration of multipolar neurons in the developing neocortex. Nat Neurosci. 2011; 14:697–703. [PubMed: 21516100]

Kalluri R, Neilson EG. Epithelial-mesenchymal transition and its implications for fibrosis. J Clin Invest. 2003; 112:1776–84. [PubMed: 14679171]

Kalluri R, Weinberg RA. The basics of epithelial-mesenchymal transition. J Clin Invest. 2009; 119:1420–8. [PubMed: 19487818]

Kim C, Ye F, Ginsberg MH. Regulation of integrin activation. Annu Rev Cell Dev Biol. 2011; 27:321–45. [PubMed: 21663444]

Knox AL, Brown NH. Rap1 GTPase regulation of adherens junction positioning and cell adhesion. Science. 2002; 295:1285–8. [PubMed: 11847339]

Kooistra MR, Dube N, Bos JL. Rap1: a key regulator in cell-cell junction formation. J Cell Sci. 2007; 120:17–22. [PubMed: 17182900]

Lampugnani MG, Orsenigo F, Rudini N, Maddaluno L, Boulday G, Chapon F, Dejana E. CCM1 regulates vascular-lumen organization by inducing endothelial polarity. J Cell Sci. 2010; 123:1073–80. [PubMed: 20332120]

Lang RA, Herman K, Reynolds AB, Hildebrand JD, Plageman TF Jr. p120-catenin-dependent junctional recruitment of Shroom3 is required for apical constriction during lens pit morphogenesis. Development. 2014; 141:3177–87. [PubMed: 25038041]

Lee HS, Lim CJ, Puzon-McLaughlin W, Shattil SJ, Ginsberg MH. RIAM activates integrins by linking talin to ras GTPase membrane-targeting sequences. J Biol Chem. 2009; 284:5119–27. [PubMed: 19098287]

Leong L, Menko AS, Grunwald GB. Differential expression of N- and B-cadherin during lens development. Invest Ophthalmol Vis Sci. 2000; 41:3503–10. [PubMed: 11006245]

Li Y, Yan J, De P, Chang HC, Yamauchi A, Christopherson KW 2nd, Paranavitana NC, Peng X, Kim C, Munugalavadla V, et al. Rap1a null mice have altered myeloid cell functions suggesting distinct roles for the closely related Rap1a and 1b proteins. J Immunol. 2007; 179:8322–31. [PubMed: 18056377]

Liu JJ, Stockton RA, Gingras AR, Ablooglu AJ, Han J, Bobkov AA, Ginsberg MH. A mechanism of Rap1-induced stabilization of endothelial cell–cell junctions. Mol Biol Cell. 2011; 22:2509–19. [PubMed: 21633110]

Lovicu FJ, McAvoy JW. Growth factor regulation of lens development. Dev Biol. 2005; 280:1–14. [PubMed: 15766743]

Maddala R, Chauhan BK, Walker C, Zheng Y, Robinson ML, Lang RA, Rao PV. Rac1 GTPase-deficient mouse lens exhibits defects in shape, suture formation, fiber cell migration and survival. Dev Biol. 2011a; 360:30–43. [PubMed: 21945075]

Maddala R, Reneker LW, Pendurthi B, Rao PV. Rho GDP dissociation inhibitor-mediated disruption of Rho GTPase activity impairs lens fiber cell migration, elongation and survival. Dev Biol. 2008; 315:217–31. [PubMed: 18234179]

Maddala R, Skiba NP, Lalane R 3rd, Sherman DL, Brophy PJ, Rao PV. Periaxin is required for hexagonal geometry and membrane organization of mature lens fibers. Dev Biol. 2011b; 357:179–90. [PubMed: 21745462]

Mamuya FA, Wang Y, Roop VH, Scheiblin DA, Zajac JC, Duncan MK. The roles of alphaV integrins in lens EMT and posterior capsular opacification. J Cell Mol Med. 2014; 18:656–70. [PubMed: 24495224]

Mandai K, Rikitake Y, Shimono Y, Takai Y. Afadin/AF-6 and canoe: roles in cell adhesion and beyond. Prog Mol Biol Transl Sci. 2013; 116:433–54. [PubMed: 23481206]

Mandell KJ, Babbin BA, Nusrat A, Parkos CA. Junctional adhesion molecule 1 regulates epithelial cell morphology through effects on beta1 integrins and Rap1 activity. J Biol Chem. 2005; 280:11665–74. [PubMed: 15677455]

Manthey AL, Lachke SA, FitzGerald PG, Mason RW, Scheiblin DA, McDonald JH, Duncan MK. Loss of Sip1 leads to migration defects and retention of ectodermal markers during lens development. Mech Dev. 2014; 131:86–110. [PubMed: 24161570]

McAvoy JW, Chamberlain CG, de Iongh RU, Hales AM, Lovicu FJ. Lens development. Eye (Lond). 1999; 13(Pt 3b):425–37. [PubMed: 10627820]

Meng W, Takeichi M. Adherens junction: molecular architecture and regulation. Cold Spring Harb Perspect Biol. 2009; 1:a002899. [PubMed: 20457565]

Menko AS, Bleaken BM, Libowitz AA, Zhang L, Stepp MA, Walker JL. A central role for vimentin in regulating repair function during healing of the lens epithelium. Mol Biol Cell. 2014; 25:776–90. [PubMed: 24478454]

Mitic LL, Anderson JM. Molecular architecture of tight junctions. Annu Rev Physiol. 1998; 60:121–42. [PubMed: 9558457]

Nelson WJ. Remodeling epithelial cell organization: transitions between front-rear and apical-basal polarity. Cold Spring Harb Perspect Biol. 2009; 1:a000513. [PubMed: 20066074]

Nieto MA. Epithelial plasticity: a common theme in embryonic and cancer cells. Science. 2013; 342:1234850. [PubMed: 24202173]

Noda M. Structures and functions of the K rev-1 transformation suppressor gene and its relatives. Biochim Biophys Acta. 1993; 1155:97–109. [PubMed: 8504133]

O'Keefe DD, Gonzalez-Nino E, Edgar BA, Curtiss J. Discontinuities in Rap1 activity determine epithelial cell morphology within the developing wing of Drosophila. Dev Biol. 2012; 369:223–34. [PubMed: 22776378]

Ogita H, Takai Y. Activation of Rap1, Cdc42, and rac by nectin adhesion system. Methods Enzymol. 2006; 406:415–24. [PubMed: 16472674]

Ooshio T, Kobayashi R, Ikeda W, Miyata M, Fukumoto Y, Matsuzawa N, Ogita H, Takai Y. Involvement of the interaction of afadin with ZO-1 in the formation of tight junctions in Madin-Darby canine kidney cells. J Biol Chem. 2010; 285:5003–12. [PubMed: 20008323]

Pan BX, Vautier F, Ito W, Bolshakov VY, Morozov A. Enhanced corticoamygdala efficacy and suppressed fear in absence of Rap1. J Neurosci. 2008; 28:2089–98. [PubMed: 18305243]

Pannekoek WJ, Kooistra MR, Zwartkruis FJ, Bos JL. Cell-cell junction formation: the role of Rap1 and Rap1 guanine nucleotide exchange factors. Biochim Biophys Acta. 2009; 1788:790–6. [PubMed: 19159611]

Pontoriero GF, Smith AN, Miller LA, Radice GL, West-Mays JA, Lang RA. Co-operative roles for E-cadherin and N-cadherin during lens vesicle separation and lens epithelial cell survival. Dev Biol. 2009; 326:403–17. [PubMed: 18996109]

Potla U, Ni J, Vadaparampil J, Yang G, Leventhal JS, Campbell KN, Chuang PY, Morozov A, He JC, D'Agati VD, et al. Podocyte-specific RAP1GAP expression contributes to focal segmental glomerulosclerosis-associated glomerular injury. J Clin Invest. 2014; 124:1757–69. [PubMed: 24642466]

Puisieux A, Brabletz T, Caramel J. Oncogenic roles of EMT-inducing transcription factors. Nat Cell Biol. 2014; 16:488–94. [PubMed: 24875735]

Raaijmakers JH, Bos JL. Specificity in Ras and Rap signaling. J Biol Chem. 2009; 284:10995–9. [PubMed: 19091745]

Rikitake Y, Mandai K, Takai Y. The role of nectins in different types of cell-cell adhesion. J Cell Sci. 2012; 125:3713–22. [PubMed: 23027581]

Sawyer JK, Harris NJ, Slep KC, Gaul U, Peifer M. The Drosophila afadin homologue Canoe regulates linkage of the actin cytoskeleton to adherens junctions during apical constriction. J Cell Biol. 2009; 186:57–73. [PubMed: 19596848]

Severson EA, Lee WY, Capaldo CT, Nusrat A, Parkos CA. Junctional adhesion molecule A interacts with Afadin and PDZ-GEF2 to activate Rap1A, regulate beta1 integrin levels, and enhance cell migration. Mol Biol Cell. 2009; 20:1916–25. [PubMed: 19176753]

Shaul YD, Freinkman E, Comb WC, Cantor JR, Tam WL, Thiru P, Kim D, Kanarek N, Pacold ME, Chen WW, et al. Dihydropyrimidine accumulation is required for the epithelial-mesenchymal transition. Cell. 2014; 158:1094–109. [PubMed: 25171410]

Shintani Y, Fukumoto Y, Chaika N, Svoboda R, Wheelock MJ, Johnson KR. Collagen I-mediated up-regulation of N-cadherin requires cooperative signals from integrins and discoidin domain receptor 1. J Cell Biol. 2008; 180:1277–89. [PubMed: 18362184]

Spahn P, Ott A, Reuter R. The PDZ-GEF protein Dizzy regulates the establishment of adherens junctions required for ventral furrow formation in Drosophila. J Cell Sci. 2012; 125:3801–12. [PubMed: 22553205]

Stump RJ, Lovicu FJ, Ang SL, Pandey SK, McAvoy JW. Lithium stabilizes the polarized lens epithelial phenotype and inhibits proliferation, migration, and epithelial mesenchymal transition. J Pathol. 2006; 210:249–57. [PubMed: 16924593]

Sugiyama Y, Akimoto K, Robinson ML, Ohno S, Quinlan RA. A cell polarity protein aPKClambda is required for eye lens formation and growth. Dev Biol. 2009; 336:246–56. [PubMed: 19835853]

Suzuki A, Ohno S. The PAR-aPKC system: lessons in polarity. J Cell Sci. 2006; 119:979–87. [PubMed: 16525119]

Thiery JP, Acloque H, Huang RY, Nieto MA. Epithelial-mesenchymal transitions in development and disease. Cell. 2009; 139:871–90. [PubMed: 19945376]

Turner CE. Paxillin and focal adhesion signalling. Nat Cell Biol. 2000; 2:E231–6. [PubMed: 11146675]

Yamben IF, Rachel RA, Shatadal S, Copeland NG, Jenkins NA, Warming S, Griep AE. Scrib is required for epithelial cell identity and prevents epithelial to mesenchymal transition in the mouse. Dev Biol. 2013; 384:41–52. [PubMed: 24095903]

Highlights

- Rap1 deficiency impairs lens morphogenesis and polarity establishment
- Rap1 deficiency disrupts lens AJs, TJs and cell-ECM interactions
- Rap1 deficiency induces EMT in mouse lens
- Rap1 deficiency impairs cell cycle progression, proliferation and survival

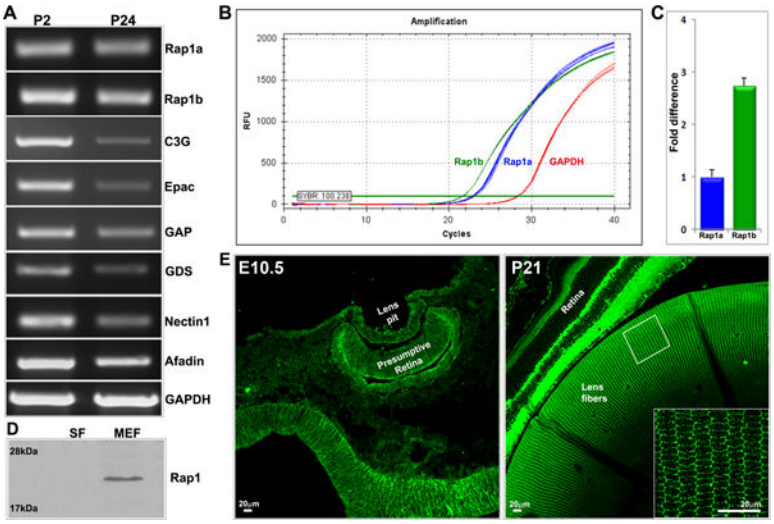

Fig. 1.

Expression and distribution profile of Rap1 GTPase and its effectors in mouse lens. A. RT-PCR analysis-based assessment of expression of Rap1a and Rap1b and their different effector and interacting proteins in P2 and P24 mouse lenses, using GAPDH expression for cDNA normalization. B & C show the qRT-PCR amplification traces for Rap1a and Rap1b expression relative to GAPDH, and the relative fold difference in expression in P2 mouse lenses, respectively. D. Distribution of Rap1 (Rap1a/Rap1b) protein in the soluble fraction (SF) and membrane enriched fraction (MEF) of P24 mouse lens based on immunoblotting analysis. E. Distribution of Rap1 in the developing (embryonic day10.5) and P21 mouse lens based on immunofluorescence analysis. The smaller rectangular box in the right panel is a magnification of the area shown as an inset. In the mature lens fibers (insert) Rap1 is localized predominantly at the cell membrane. In panel C, the error bar indicates SEM based on values derived from three independent analyses. In panel E bars represent image magnification.

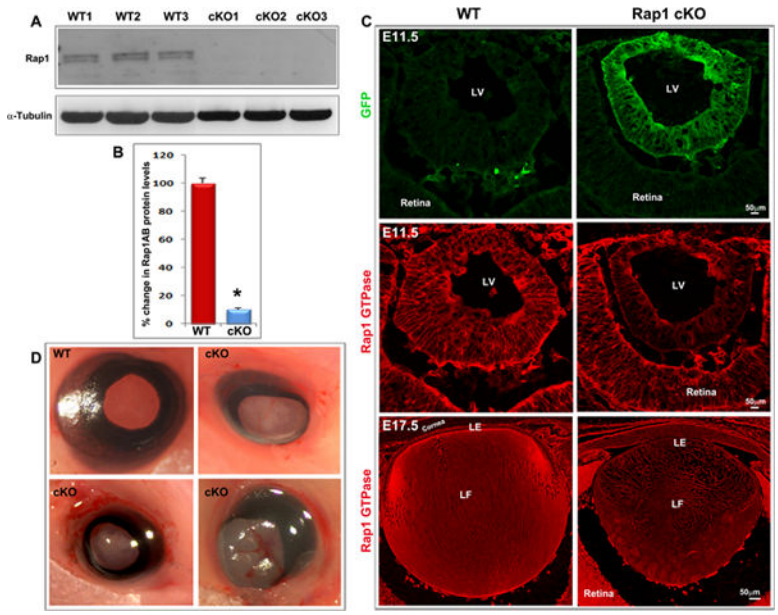

Fig. 2.

Ocular phenotype in the Rap1 cKO mouse. A & B. Intact lenses (membrane-enriched fraction) derived from three representative E17.5 Rap1 cKO mouse embryos showed a dramatic reduction (by ~ 90%; *P<0.05; n=4) of Rap1 (Rap1a/Rap1b-total) protein compared with WT controls based on immunoblot quantification. C. Reduction of Rap1 in lenses from E11.5 and E17.5 Rap1 cKO mouse embryos based on immunofluorescence analysis. The top panel shows the distribution profile of GFP (green fluorescent protein) only in the lens vesicle of Rap1 cKO mouse embryos (E11.5) confirming Cre expression relative to the WT control. The middle and lower panels show reduction of Rap1 in the E11.5 lens vesicle and E17.5 lens, respectively, derived from Rap1 cKO mice and relative to the WT controls based on immunofluorescence analysis. D. Conditional deletion of Rap1 (Rap1a/Rap1b) in the lens results in microphthalmic eyes with lens opacity in the embryonic and neonatal mice. The images shown are with eye lids removed from the E17.5 embryos. Bars in panel C represent image magnification. LV: Lens vesicle; LE: Lens epithelium; LF: Lens fibers.

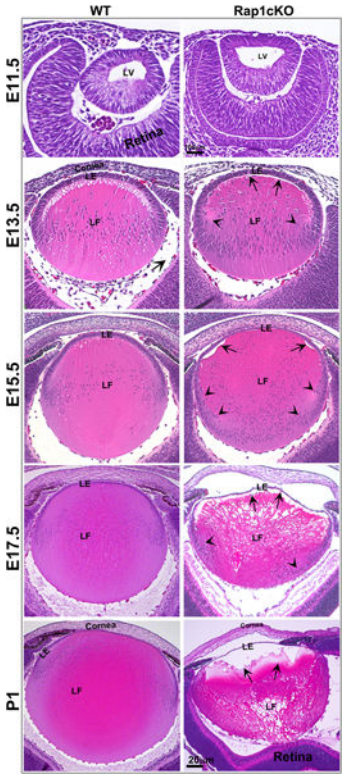

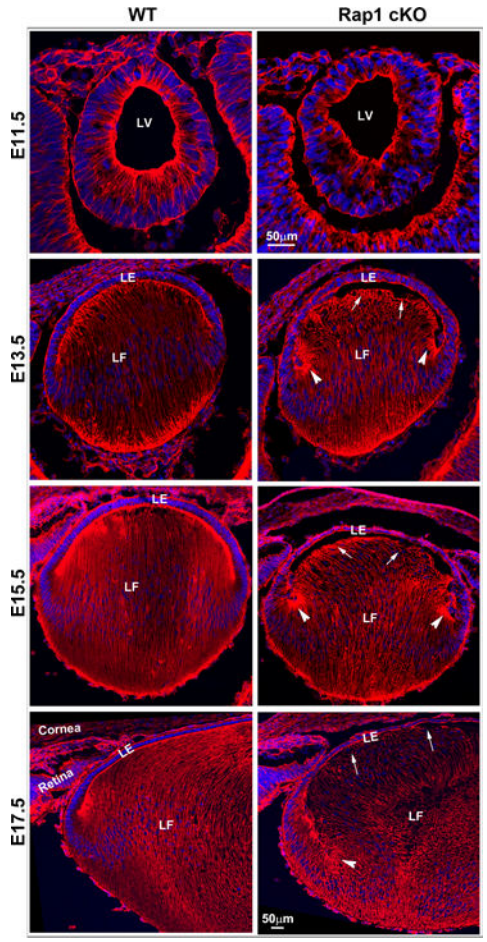

Fig. 3.

Histological and actin cytoskeletal changes in the developing and neonatal Rap1 cKO mouse eye. A. To determine the effects of conditional Rap1 deficiency on lens changes during development, ocular specimens derived from the E11.5, 13.5, 15.5, 17.5 embryos and day 1 neonatal Rap1 cKO mice were fixed, sectioned and stained with H&E. The tissue sections were imaged using a light microscope. Although the lens vesicle in E11.5 Rap1 cKO mouse embryos showed no overt changes in formation and separation, starting from E13.5 to P1, there was a progressive disruption in fiber cell apical attachment with lens epithelial apical ends (indicated with arrows), resulting in an empty space between the epithelium and fibers in Rap1 cKO specimens compared with WT controls. In E17.5 and P1 Rap1 cKO lenses, there was a gross disorganization of fibers with noticeable disruption at the lens fulcrum (arrow heads) compared with WT controls. In E13.5 specimens derived from the Rap1 cKO embryos, fiber cell migration pattern at the fulcrum is noticeably different from the WT controls (arrow heads) and in E15.5 and 17.5 specimens, the nuclei spread to below the transitional zone and are retained at the posterior ends of the fibers (arrow heads). B. To further evaluate lens defects in the Rap1 cKO mice, cryotissue sections derived from the E11.5 to E17.5 stages from Rap1 cKO and WT mice described above were stained for F-actin with rhodamine phalloidin, prior to image capture by confocal microscopy. Similar to the histological changes noted in Fig. 3A, defective cell-cell attachment between the lens

epithelial apical ends and fiber cell apical ends was clearly noted in embryonic Rap1 cKO mouse specimens, in E13.5 and 15.5 specimens, and is indicated with arrows. Additionally, arrow heads indicate defects in the lens fulcrum formation in E13.5 and E15.5 Rap1 cKO embryos. F-actin distribution in the lens vesicle at the apical ends of cells shows reduced staining and extending a similar reduction at the apical junctions of epithelial and fiber cells in E13. 5, 15.5 and 17.5 specimens in the Rap1 cKO embryos compared with WT controls. In E17.5 Rap1 cKO lens specimens, there is a gross disruption in fiber cell organization compared with WT controls. LV: Lens vesicle, LE: Lens epithelium, LF: Lens fibers. Bars in A and B represent image magnification.

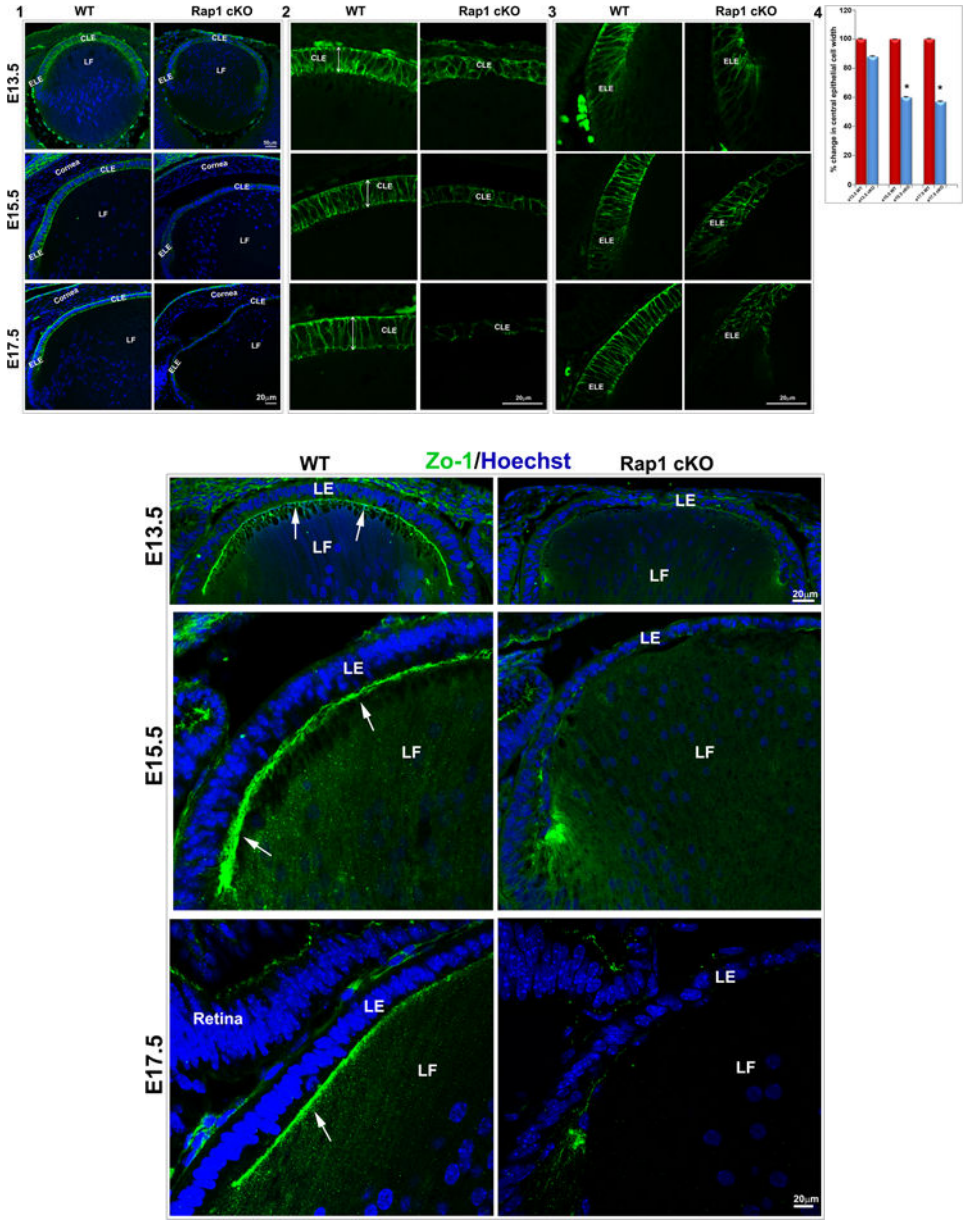

Fig. 4.

Disruption of E-cadherin-based AJs and ZO-1associated cell-cell interactions in Rap1 cKO mouse lenses. A. The Rap1 cKO mouse specimens derived from E13.5, 15.5 and 17.5 embryos reveal a progressive disruption in E-cadherin based AJs (green) in lens epithelium associated with altered cell shape and significantly reduced cell width compared to the respective WT controls (A1, A4). While lens epithelial cells (in both central (A2) and equatorial (A3) epithelium) in WT specimens exhibit a long columnar shape (double headed arrow; known to depend on maintenance of apical to basal polarity) and intense E-cadherin-positive AJs, the Rap1 cKO lens specimens exhibit a dramatic reduction in E-cadherin-based AJs both in central (A2) and equatorial (A3) epithelium, and disruption of apical to basal polarity with altered cell shape. A4 shows a significant decrease in lens central epithelial width in the Rap1 cKO specimens compared with WT, based on values (mean ± SEM)

derived from 6 independent specimens. *P<0.05. LE: Lens epithelium, LF: Lens fibers, CLE: Central lens epithelium, ELE: Equatorial lens epithelium. B. Similar to AJs shown in Fig. 4A, ZO-1-based cell adhesive interactions were dramatically reduced in the lens of E13.5, E15.5 and E17.5 Rap1 cKO embryos. ZO-1 based cell-cell interactions (in green) were distributed discretely between the apical junctions of fiber cells and epithelium in the WT lenses (arrows). However, in the absence of Rap1, the ZO-1 based cell-cell interactions were dramatically reduced. The loss of cell adhesive interactions was associated with reduction in number and size of nuclei in the lens epithelium of Rap1 cKO specimens relative to WT controls, based on Hoechst staining (blue). Bars represent magnification.

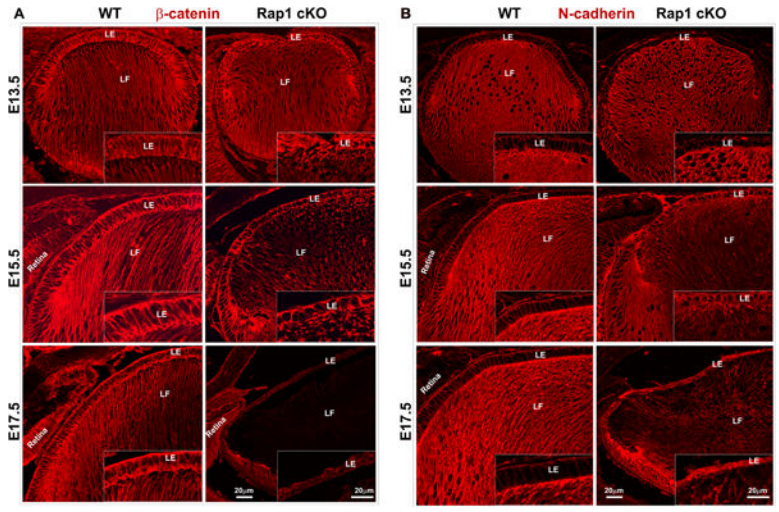

Fig. 5.

Rap1 deficiency suppresses β-catenin-based cell-cell junctions and increases N-cadherin levels in mouse lens epithelium. A. β-catenin, a well-characterized component of AJs localizes to the cell-cell junctions of lens epithelium and fiber cells in WT specimens based on immunofluorescence analysis (red) of paraffin embedded sagittal sections. In Rap1 cKO E13.5, E15.5 and E17.5 specimens, there is a progressive and dramatic reduction of β-catenin staining in both lens epithelium and fibers compared to WT specimens. The insets show magnified areas of lens epithelium. B. Unlike β-catenin, N-cadherin distribution (red staining) is relatively intense in fiber cells compared to the epithelium of WT lenses of mouse embryos. However, in the Rap1 cKO mouse lens specimens (E13.5, 15.5 and 17.5), there was a progressive and marked increase in N-cadherin staining in the epithelium with a dramatic and concomitant reduction in the fiber cells. The insets show the magnified area of lens epithelium. Bars represent image magnification. LE: Lens epithelium, LF: Lens fibers.

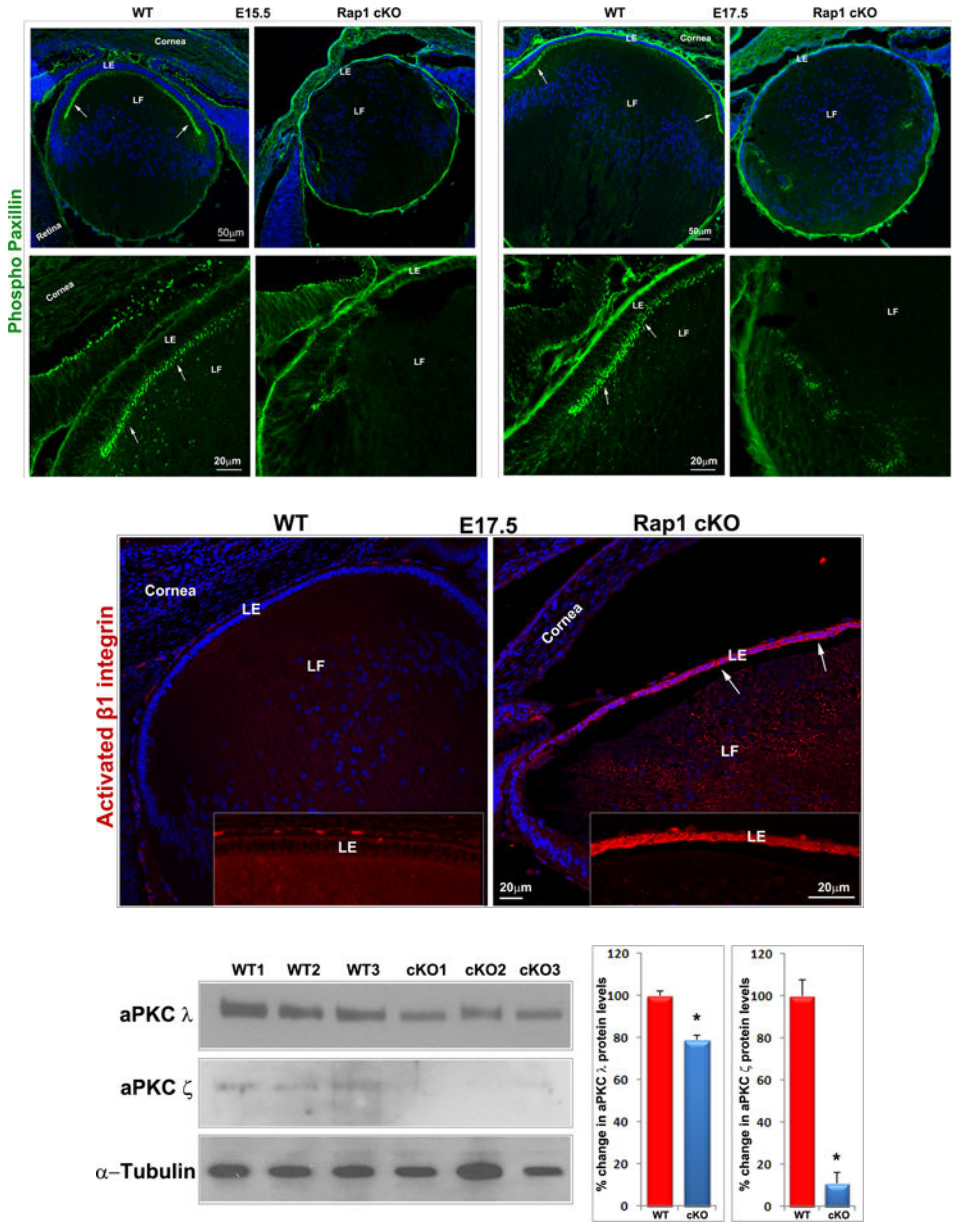

Fig. 6.

Rap1 deficiency disrupts cell-ECM adhesion, β1 integrin activation and PAR complex in mouse lens. A. To determine the influence of Rap1 deficiency on cell-ECM interactions, E15.5 and E17.5 ocular specimens derived from the Rap1 cKO embryos were evaluated for changes in activation status of paxillin based on immunofluorescence analysis of phosphorylation (Tyr118) status. In WT specimens, phospho-paxillin (green) is distributed discretely and intensely to the apical junction of epithelial and fiber cells (arrows) very similar to the distribution pattern of ZO-1. Lens capsule (both anterior and posterior) also appears to exhibit some positive staining. In Rap1 cKO (E15.5 and E17.5) mouse ocular specimens, a dramatic reduction in phospho-paxillin staining is noted at the apical junctions of epithelial and fiber cells compared with WT controls. B. Immunofluorescence analysis shows that weak staining for β1-integrin (detected using a monoclonal antibody which

recognizes the activated epitope of β1-integrin) was found to be distributed throughout the WT lens, in both the epithelium and fibers (red). These specimens were also labeled for cell nuclei using Hoechst (blue). In contrast, the lens epithelium of Rap1 cKO mouse embryos showed a robust increase in β1-integrin specific staining (arrows). In lens fibers of Rap1 cKO mouse embryos, there appears to be some decrease in the staining for β1-integrin relative to WT controls. Insets depict magnified areas of the central epithelium. Bars in both A and B represent image magnification. LE: Lens epithelium, LF: Lens fibers. C. To determine the status of PAR complex activity in Rap1 cKO mouse lens specimens, the levels of aPKC (both aPKCλ and aPKCς), a well-characterized component of PAR, were examined by immunoblot analysis in E17.5 lenses and compared with respective WT lenses. The levels of both aPKCλ and aPKCς were decreased significantly in the Rap1 cKO lenses (total lysates) compared to WT controls. Immunoblots of three individual representative specimens from both WT and Rap1 cKO are shown. α-tubulin was immunoblotted as a loading control.

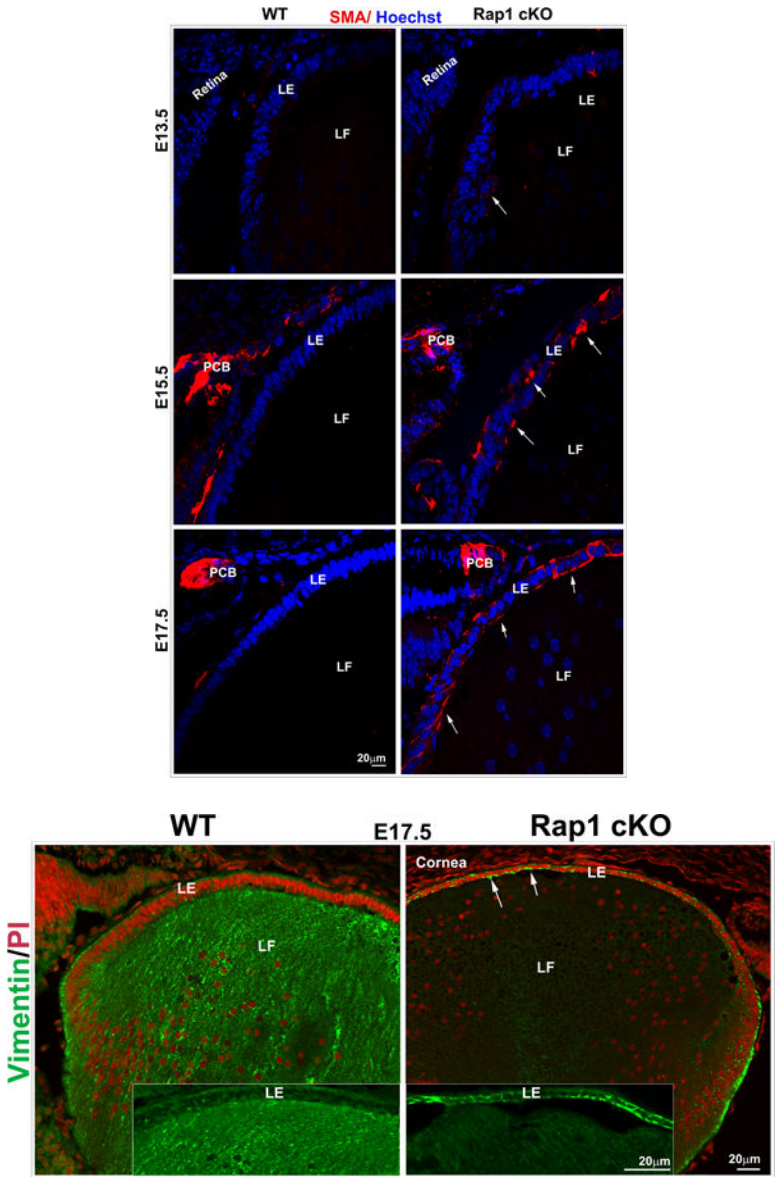

Fig. 7.

Rap1 deficiency induces EMT in mouse lens. A. To determine the effects of Rap1 deficiency on lens epithelial plasticity, E13.5, 15.5 and 17.5 ocular specimens derived from Rap1 cKO mouse embryos were evaluated for changes in αSMA by immunofluorescence analysis using an anti-αSMA monoclonal antibody conjugated with Cy3™. While the respective WT specimens show absence of αSMA in lens epithelium, the Rap1 cKO mouse lens specimens exhibit progressively increased levels of αSMA in the epithelium of E13.5, E15.5 and E17.5 specimens (indicated with arrows; red staining). Both WT and Rap1 cKO mouse specimens exhibit αSMA staining in the presumptive ciliary body (PCB) and iris. B. In addition to αSMA, changes in vimentin were examined in the Rap1 cKO mouse ocular specimens by immunofluorescence analysis. In E17.5 WT specimens, fibers stain intensely for vimentin (green) with very little positive staining in the lens epithelium (see inserts). Rap1 cKO mouse lens specimens in contrast, exhibit a marked increase in vimentin staining

in the lens epithelium (arrows), with a concomitant decrease in the fiber cells. Insets show magnified areas of lens epithelium and fibers. Red staining shows propidium iodide (PI)-based nuclei distribution. LE; Lens epithelium, LF: Lens fibers. Bars in A and B represent image magnification.

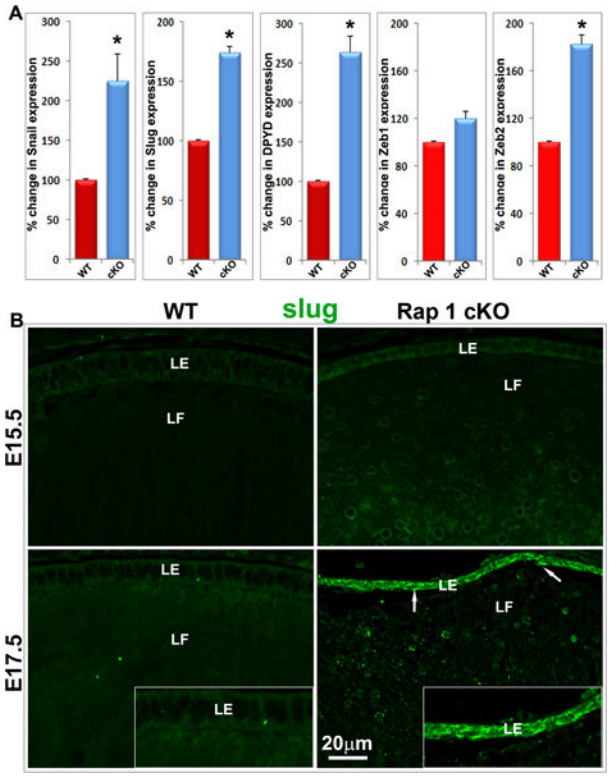

Fig. 8.

Upregulation of E-cadherin suppressing transcription factors and the mesenchymal metabolic marker dihydropyrimidine dehydrogenase (DPYD) in Rap1 cKO mouse lens. A. Lenses derived from the E17.5 Rap1 cKO mice were evaluated for changes in the expression levels of E-cadherin suppressing transcription factors including Snai1, Slug, Zeb1 and Zeb2, and DPYD, based on qRT-PCR analysis in comparison with WT controls. Rap1 cKO embryonic mouse lenses showed a significant increase in the expression of Snai1, Slug, Zeb2 and DPYD compared with WT controls. Values represent mean ± SEM. n=3 (pooled specimens). *P< 0.05. B. To further confirm the changes observed in the expression of E-cadherin suppressing transcription factors, changes in Slug protein distribution was evaluated by immunofluorescence analysis in the E15.5 and E17.5 ocular specimens derived from the Rap1 cKO mouse embryos in comparison with WT controls. Slug protein levels markedly and progressively increased in the epithelium (arrows, green staining) of E15.5 and E17.5 Rap1 cKO specimens. There was also some increase of Slug protein in the fiber cells of Rap1 cKO mouse lens compared with WT controls. Insets show a magnified area of lens epithelium. LE: Lens epithelium; LF: Lens fibers. Bar represents image magnification.

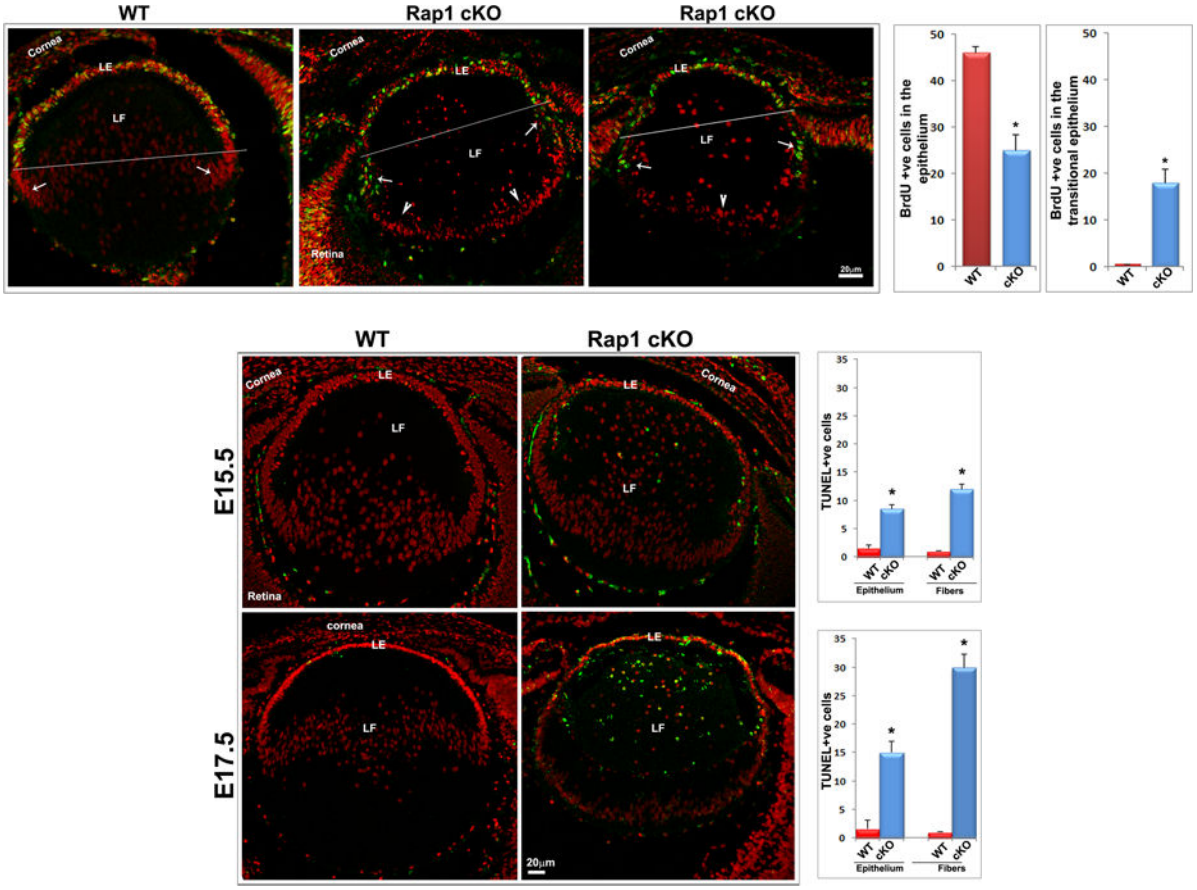

Fig. 9.

Rap1 deficiency impairs lens epithelial proliferation and survival. A. To determine the effects of Rap1 deficiency on lens epithelial proliferation and cell cycle progression, in vivo BrdU labeling was performed in conjunction with immunofluorescence analysis using anti-BrdU antibody as described in Methods section. Counting of BrdU positive cells showed a significant decrease (>50%) in the lens central epithelium of Rap1 cKO embryos relative to their WT controls. In contrast to the lens central epithelium, no BrdU-positive cells are noted in the transitional zone of the WT epithelium, where cells exit from the cell cycle and start differentiating into secondary fiber cells (a region just below the line drawn and indicated with arrows). Rap1 cKO mouse lens specimens on the other hand, exhibited a significant increase in the number of BrdU positive cells in the transitional zone epithelium (arrows) indicating defective cell cycle exit in the deficiency of Rap1. B. To test the effects of Rap1 deficiency on lens epithelial and fiber cell survival, we examined for changes in apoptotic cells by TUNEL positive staining of ocular specimens in E15.5 and E17.5 mouse embryos. The Rap1 cKO mouse specimens showed a progressively and significantly increase of apoptotic cells (TUNEL positive cells- in green/yellow) in the lens epithelium and fiber mass compared with WT controls. Values (mean ± SEM) were based on n=6. *P<0.05. Bars show image magnification. LE: Lens epithelium, LF: Lens fibers.

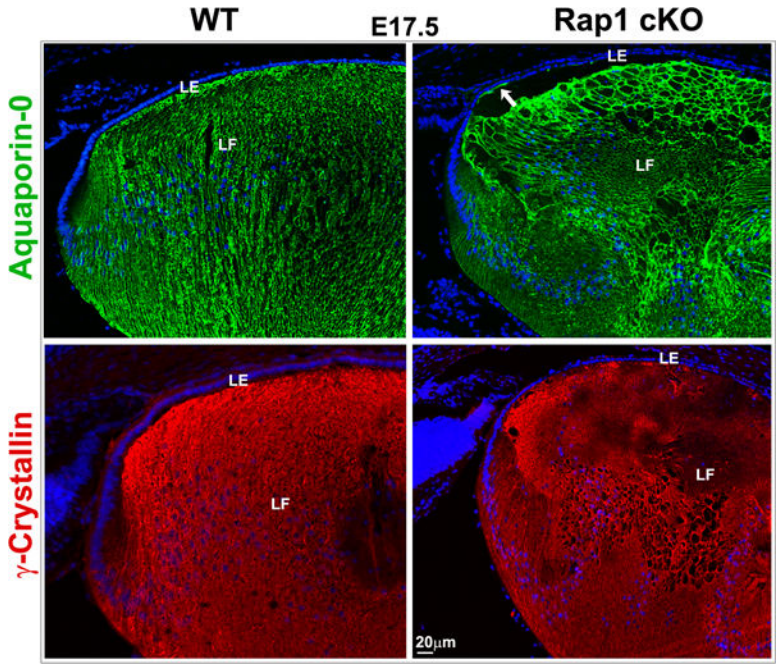

Fig. 10.

Lens differentiation is normal under Rap1 deficiency. To test whether Rap1 deficiency influences lens differentiation, E17.5 ocular specimens derived from Rap1 cKO mouse embryos along with their respective WT specimens were examined by immunofluorescence analysis for expression profile of lens fiber specific markers including aquaporin-0 (green) and γ-crystallin (red). As shown in the figure, the distribution profile of various fiber cell differentiation markers was found to be comparable between the Rap1 cKO and WT specimens, indicating that Rap1 deficiency does not impact normal lens differentiation. In some Rap1 cKO specimens, there was aquaporin-0 positive staining at the apical surface of lens epithelium as indicated by the arrows. Bar represents image magnification. LE: Lens epithelium, LF: Lens fibers.